CHAPTER 19

Photoactive Self-Assembled Monolayers (SAMs)

Toshihiro Kondo[1], Kohei Uosaki[2]

[1]*Department of Chemistry, Faculty of Science, Ochanomizu University, 2-1-1, Ohtsuka, Bunkyo-ku, Tokyo 112-8610, Japan*
[2]*Physical Chemistry Laboratory, Division of Chemistry, Graduate School of Science, Hokkaido University, Sapporo 060-0810, Japan*

CONTENTS

1. INTRODUCTION

Photoactivity is one of the most important functionalities for constructing molecular devices. Construction of highly efficient molecular photodevices should require the arrangement of molecules in order at a molecular level because the photoinduced electron/energy transfer between molecules and the structure and/or the properties of molecules are changed by photoperturbation. As described in this book [Vol. 3, Ch. 14], one of the most important techniques in modern nanotechnology is the arrangement of molecules in order on a solid surface with a nanometer precision, and the self-assembly (SA) technique has become a widely used method for constructing ordered molecular layers, because molecules in self-assembled monolayers (SAMs) are chemisorbed onto the solid surface and are therefore expected to be stable. SAMs of alkylthiols on metals, especially on gold, have been extensively studied because of their potential applications in many fields, such as sensors, wetting control, and biomolecular and molecular electronic devices [1–5]. Thus, alkylthiol SAMs with several functionalities have been extensively investigated by many research groups, including our group, since the 1990s [1–46] and are one of the best candidates for construction of highly efficient molecular photodevices. Although there is another type of SAMs constructed using the silane coupling reaction of alkoxysilane on an oxide surface [1, 2], here we concentrate only on alkylthiol SAMs as in this book [Vol. 3, Ch. 14]. In that chapter, the method for constructing alkylthiol SAMs on a metal surface and the structures of the SAMs during their process of formation and after their formation were described in detail. In this chapter, we focus on and review various photo-characteristics of SAMs: photoinduced electron transfer at electrodes modified with SAMs and at electrodes modified with a nanocluster modified with SAMs, control of photoelectrochemical properties by the SAMs, control of electron transfer by photoisomerization

ISBN: 1-58883-083-7

Bottom-Up Nanofabrication
Edited by Katsuhiko Ariga and Hari Singh Nalwa
Volume 4: Pages: 409–424

at the SAMs, application of luminescence from the SAMs, especially to sensors, and making micro/nanopatterns using the SAMs.

2. PHOTOINDUCED ELECTRON TRANSFER AT SAMs

Construction of a very efficient artificial photoelectric conversion device mimicking a natural photosynthetic system is one of the dreams of scientists. In natural systems, molecules of various functionalities, such as a photon absorber like chlorophylls and electron donors and acceptors like pheophytins and quinones, are well-organized with molecular dimensions such that very efficient photoinduced charge separation and photoinduced electron transfer are achieved with a minimum reverse electron transfer [47, 48]. Thus, it is of great interest to mimic the elaborate molecular machinery of natural systems for the realization of a highly efficient artificial photosynthetic system. This concept was first employed by Moore et al. and Fujihira et al., who used lipid bilayer membranes [49, 50] and Langmuir-Blodgett (LB) films [51–55], respectively, to arrange molecules in order. Unfortunately, the quantum efficiencies of these systems were quite low (0.4–1.5%) [49, 50] compared with those of natural systems because the molecular arrangements of these systems were not high enough to achieve a highly efficient photoinduced electron transfer.

In order to achieve a highly efficient photoinduced electron transfer, the order of molecules in the films should be required with a molecular dimension as described above, and then alkylthiol SAMs on gold can be employed as a method for constructing a molecular system based on the concept shown in Figure 1, where the metal electrode is modified with a SAM containing a photon absorber, electron relay, and surface-active groups. Based on this concept, we have achieved for the first time the construction of alkylthiol SAMs for an artificial photosynthetic system using porphyrin-quinone-thiol (PQSH) and porphyrin-ferrocene-thiol (PFcSH) coupling molecules as shown in Figure 2, parts (a) and (b), respectively [56–58]. PQSH with porphyrin as the photon absorber, quinone as the electron relay, and thiol as the surface-active group was synthesized. PFcSH, which has porphyrin, ferrocene, and thiol groups as the photoactive, electron transport or relay, and surface-binding groups, respectively, separated from each other by alkyl chains, was also synthesized. Then their SAMs were constructed on a gold surface. Figure 3 shows cyclic voltammograms (CVs) at gold electrodes modified with SAMs of PQSH and PFcSH. In both curves, a pair of redox waves due to the redox reaction of quinone and ferrocene groups were observed at +210 mV (vs. Ag/AgCl) and +610 mV, respectively. From the charges of their waves, the amounts of surface-bound molecules were estimated to be 3.7×10^{13} and 1.4×10^{14} molecules cm^{-2} at PQSH and PFcSH SAMs, respectively. The difference in the surface coverage of PQSH and PFcSH should be caused by the presence of alkyl chains in the PFcSH SAM. The orders of the molecular layer of PFcSH should be higher than that of PQSH. When gold electrodes modified with SAMs of PQSH and PFcSH were illuminated in electrolyte solutions containing methylviologen (MV^{2+}) as an electron acceptor, a stable cathodic photocurrent flowed if the electrode potentials were more negative than +200 and +650 mV, respectively, which coincide with the redox potentials of the quinone and ferrocene moieties in the SAMs, respectively (Fig. 4). It is noted here that the illumination at the PQSH SAM was a white light (15 mW cm^{-2}) from the Xe lamp,

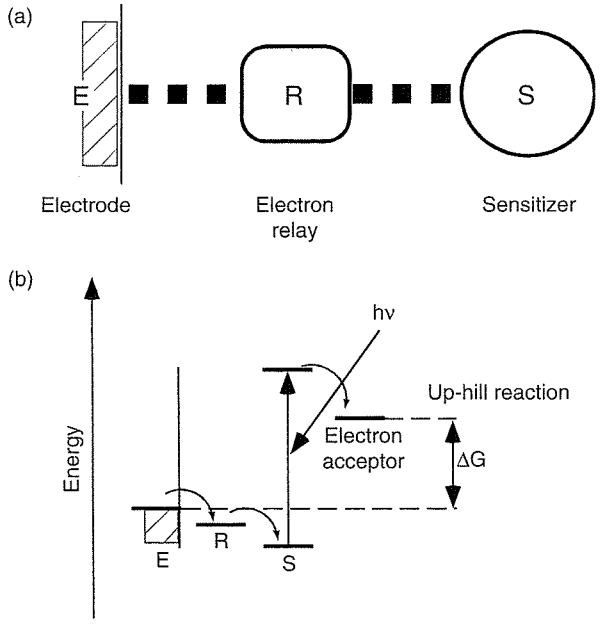

Figure 1. (a) Molecular scheme of the concept to attain highly efficient photoinduced electron transfer and (b) energy diagram of this system. Reprinted with permission from [58], K. Uosaki et al., *J. Am. Chem. Soc.* 119, 8367 (1997). © 1997, American Chemical Society.

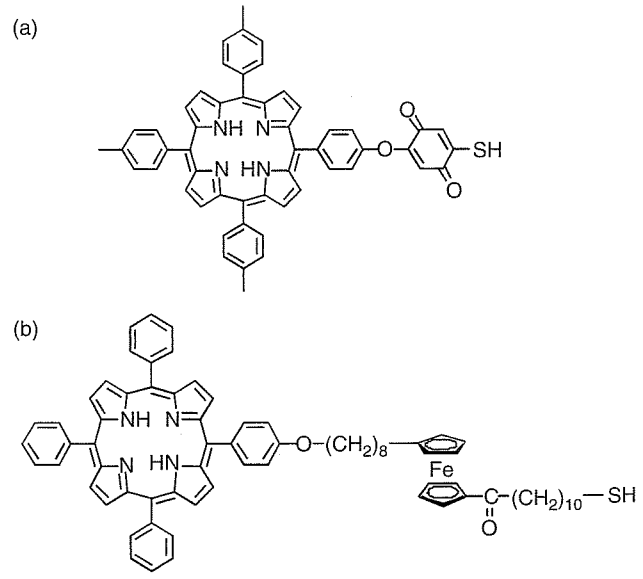

Figure 2. (a) PQSH molecule. Reprinted with permission from [56], T. Kondo et al., *Thin Solid Films* 284/285, 652 (1996). © 1996, Elsevier. (b) PFcSH molecule. Reprinted with permission from [58], K. Uosaki et al., *J. Am. Chem. Soc.* 119, 8367 (1997). © 1997, American Chemical Society.

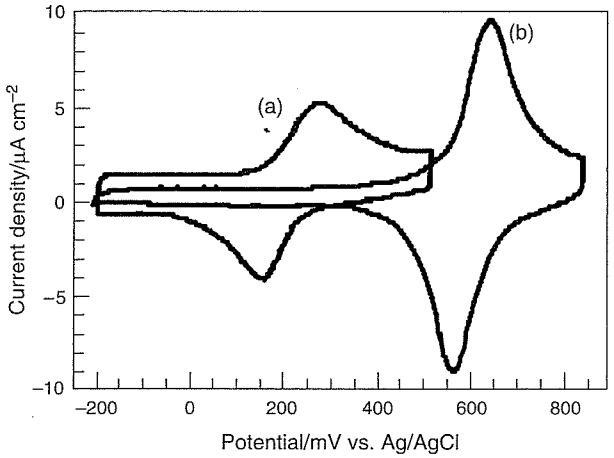

Figure 3. Cyclic voltammograms at gold electrodes modified with SAMs of (a) PQSH and (b) PFcSH measured in 0.1 M Na_2SO_4 and 0.1 M $NaClO_4$, respectively, containing 5 mM MV^{2+}. Reprinted with permission from [56], T. Kondo et al., *Thin Solid Films* 284/285, 652 (1996). © 1996, Elsevier.

while that at the PFcSH SAM was a monochromated light (430 nm, 40 $\mu W\,cm^{-2}$). These stable photocurrents flowed for many hours without any signs of deterioration. After prolonged illumination of the SAM-modified electrodes, the color of the solution in front of the electrode changed to blue, showing that MV^{2+} had been reduced to the methylviologen cation radical ($MV^{+\bullet}$). Since the redox potential of $MV^{2+}/MV^{+\bullet}$ is −630 mV, we have achieved the uphill transport of electrons of more than 0.8 eV at the PQSH SAM and more than 1.2 eV at the PFcSH SAM by visible light illumination. The photocurrent action spectra of the gold electrodes modified with the PQSH and PFcSH SAMs matched well with the absorption spectra of the PQSH and PFcSH SAMs, confirming that the porphyrin groups in both

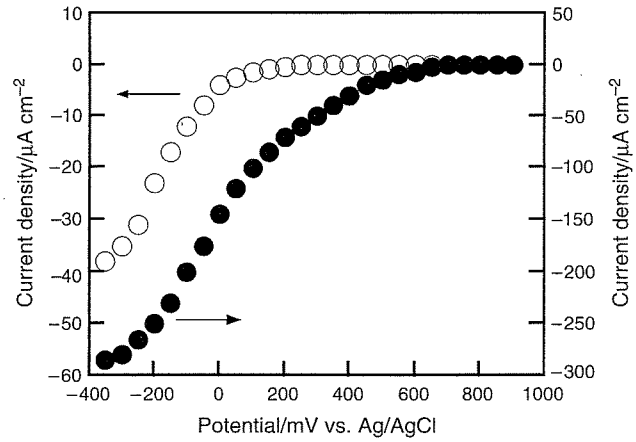

Figure 4. Potential dependence of photocurrents of (a) PQSH SAM-modified and (b) PFcSH SAM-modified gold electrodes measured in 0.1 M Na_2SO_4 and 0.1 M $NaClO_4$, respectively, containing 5 mM MV^{2+}. Reprinted with permission from [56], T. Kondo et al., *Thin Solid Films* 284/285, 652 (1996). © 1996, Elsevier; from [57], T. Kondo et al., *J. Electroanal. Chem.* 438, 121 (1997). © 1997, Elsevier; from [58], K. Uosaki et al., *J. Am. Chem. Soc.* 119, 8367 (1997). © 1997, American Chemical Society.

of the SAMs really acted as photoactive sites. The quantum efficiencies of these systems were more than 3% at the PQSH SAM and more than 10% at the PFcSH SAM. It was demonstrated by the results of the alkyl chain length dependence, a structural study by angle-resolved X-ray photoelectron spectroscopy (ARXPS), and the electrode surface

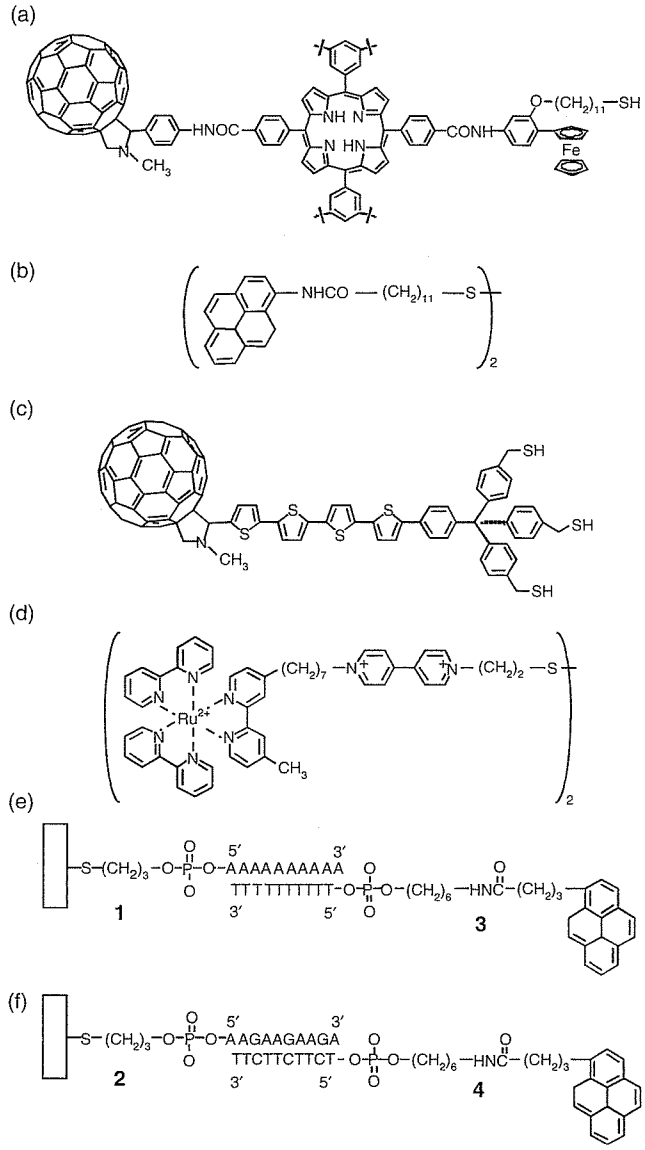

Figure 5. (a) FuPorFcSH molecule. Reprinted with permission from [62], H. Imahori et al., *J. Phys. Chem.* 104, 2009 (2000). © 2000, American Chemical Society. (b) Pyrene-thiol linked molecule. Reprinted with permission from [72], H. Imahori et al., *J. Am. Chem. Soc.* 123, 100 (2001). © 2001, American Chemical Society. (c) Fullerene-olligothiophene linked molecule. Reprinted with permission from [73], D. Hirayama et al., *J. Am. Chem. Soc.* 124, 532 (2002). © 2002, American Chemical Society. (d) $(Ru(bpy)_3^{2+})$-viologen-thiol linked molecule. Reprinted with permission from [77], T. Akiyama et al., *Jpn. J. Appl. Phys.* 41, 4737 (2002). © 2002, Japanese Applied Physics Society. (e, f) Constructed photoactive SAMs using surface-confined oligonucleotides **1** and **2**, respectively, associated with their pyrene end-labeled complements **3** and **4**, respectively. Reprinted with permission from [80], R. S. Reese and M. A. Fox, *Can. J. Chem.* 77, 1077 (1999). © 1999, National Research Council of Canada.

flatness dependence that the reason for the achievement of such a very high efficiency at the PFcSH SAM is the relatively high orientation of this SAM due to the introduction of the alkyl chain between each functional group, and then the reverse electron and energy transfer are minimized [59–61].

Following our reports, a large number of photoinduced electron transfer studies using alkylthiol SAMs have been carried out [62–79]. Imahori et al. synthesized a fullerene-porphyrin-ferrocene-thiol coupling molecule (FuPorFcSH, Fig. 5(a)), which has two electron relay groups, i.e., ferrocene and fullerene, with porphyrin placed between them as a photon absorber, and many derivatives similar to this molecule, and then constructed their SAMs on gold and indium tin oxide (ITO) [62–71]. A high efficiency of 20–25% was achieved by the SAM of FuPorFcSH. They concluded that utilization of the fullerene group with the small reorganization energy satisfies the requirement for the high photocurrent generation, leading to high efficiency even at the metal electrode. They constructed a mixed SAM with FuPorFcSH and a pyrene-thiol linked molecule (Fig. 5(b)) as an antenna group to mimic natural systems and achieved light harvesting with a photocurrent generation efficiency of 0.6–1.5% [72]. They also constructed a SAM of a fullerene-olligothiophene linked molecule (Fig. 5(c)) and observed a relatively large photocurrent [73, 74]. Ishida and Majima observed a much more intense photocurrent by surface

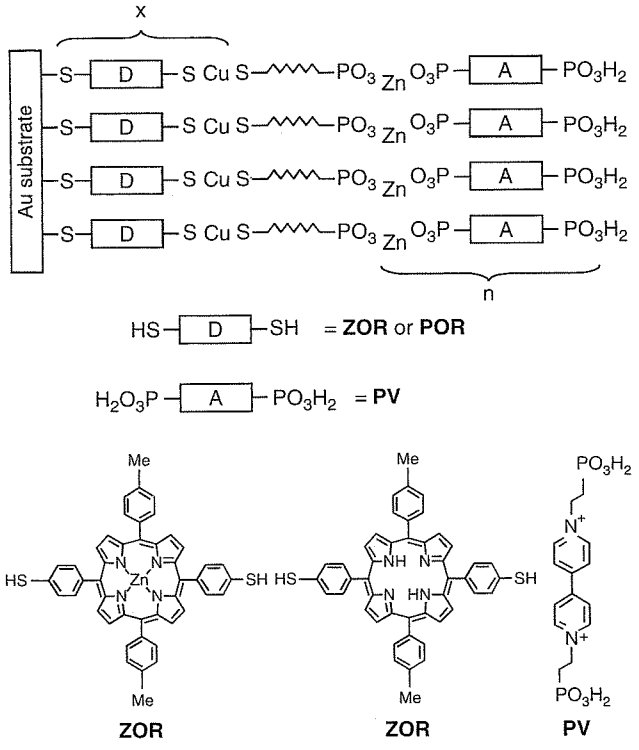

Figure 6. Top: Schematic side view of the photoactive multilayers developed by Thompson et al. using the molecules shown below. Bottom: Structures of the porphyrins and the viologen derivative used to construct the above multilayers. Reprinted with permission from [81], F. B. Abdelrazzaq et al., *J. Am. Chem. Soc.* 124, 4796 (2002). © 2002, American Chemical Society.

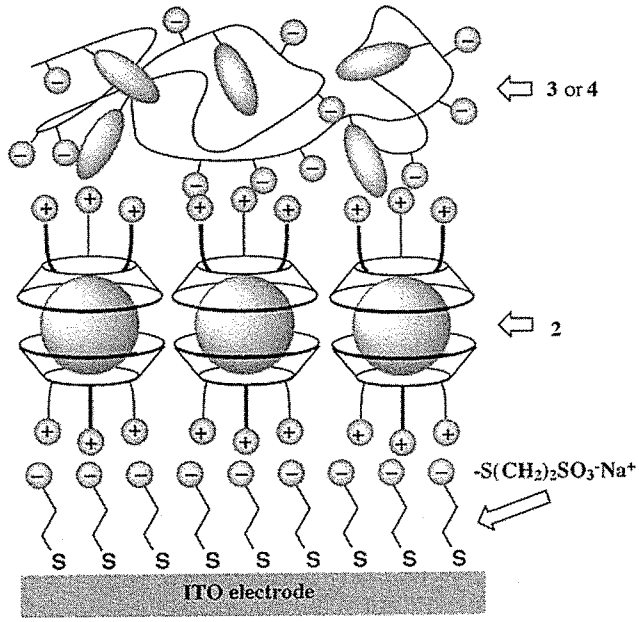

Figure 7. Schematic view of photoactive multilayers of sodium 3-mercaptoethanesulfonate (first layer), fullerene-cationic homooxacalix[3]arene inclusion complex **2** (second layer), and anionic porphyrin polymer **3** or **4** (third layer) on an ITO electrode. Reprinted with permission from [82], A. Ikeda et al., *J. Am. Chem. Soc.* 123, 4855 (2001). © 2001, American Chemical Society.

plasmon excitation than that provided by conventional direct photoexcitation at the SAM of a porphyrin-thiol linked molecule [75]. A ruthenium complex was also used as a photon absorber [76–78]. Yamada et al. constructed SAMs of a ruthenium(II) tris(2,2′-bipyridine) ($Ru(bpy)_3^{2+}$)-viologen-thiol derivative (Fig. 5(d)) on gold and ITO, and photocurrent generation was observed. There is also a report of fullerene being used as a photon absorber [79].

There are examples of photocurrent observations at a multilayer using a SAM as an underlayer. Reese and Fox constructed a SAM of a thiol-terminated oligonucleotide on gold and then constructed an oligonucleotide duplex with a pyrene end-labeled oligonucleotide on the SAM (Figs. 5(e, f)) [80]. They observed a photocurrent at this SAM-modified gold electrode in a solution containing MV^{2+} as an electron acceptor. Thompson et al. also observed photocurrent generation at photoactive multilayers constructed on a porphyrin SAM using electrostatic interaction between a zirconium cation and a phosphate anion (Fig. 6) [81]. Shinkai et al. also constructed a multilayer of a fullerene-cationic homooxacalix[3]arene inclusion complex and anionic porphyrin polymer on an ITO electrode modified with a SAM of a sulfonate-terminated thiol molecule (Fig. 7), and they observed a relatively large photocurrent [82].

3. CONTROL OF PHOTO-ELECTROCHEMICAL PROPERTIES BY SAMs

An alkylthiol SAM can also be formed on a semiconductor surface [83–89] and this SAM can control photoelectrochemical properties of the semiconductor substrates,

although it is not easy to prepare it at room temperature compared with the case of an alkylthiol SAM on a metal surface. A relatively ordered monolayer of the alkylthiol can be prepared by heating a solution containing an appropriate alkylthiol and dipping the semiconductor substrate in it for several hours. Gu and Waldeck constructed an n-InP semiconductor electrode modified with SAMs of *n*-alkylthiols having several different alkyl chain lengths and observed a photocurrent [84–88]. They investigated the alkyl chain length dependence on the photocurrent and demonstrated that studies of photocurrent versus chain length of the alkylthiols can be used to examine how the electron transfer rate constant depends on the thickness of the insulating layer. They suggested that of particular interest is the ability of the alkylthiol SAM to probe the distance dependence of the electronic coupling. The principles of photocurrent generation at semiconductor electrodes have been studied in detail and are summarized in the literatures [90–93].

4. PHOTOINDUCED ELECTRON TRANSFER AT SAM-COVERED NANOCLUSTER LAYERS

Since an alkylthiol SAM is a monomolecular film, the concentration of functional molecules is very low compared with that in a three-dimensional system, and the quantum efficiency of the SAM system is low. However, it is difficult to construct a multilayer using the SA technique because surface reaction with a relatively low yield to connect the molecules would be required. Thus, metal nanoclusters whose surfaces were covered with alkylthiol SAMs with several functional groups were employed to construct three-dimensional systems, since Brust et al. reported that alkylthiol SAM-covered gold nanoclusters are stable and that functional groups can be easily introduced by a place-exchange method [94–96]. There have been studies on photoinduced electron transfer using alkylthiol SAM-modified metal or semiconductor nanoclusters [97–112]. It should be noted here that in the case of SAM-covered semiconductor nanoclusters, the role of the SAMs play is control of the photoelectrochemical properties of the semiconductor and/or assistance in the construction of the three-dimensional system.

Yamada et al. observed photocurrents at ITO electrodes modified with a multilayer of gold nanoclusters and porphyrin-tetraalkylthiol molecules (Fig. 8) [97]. Imahori et al. investigated the photophysical properties of gold nanoclusters modified with a SAM of a porphyrin-thiol coupling molecule [98, 99], and observed a photocurrent at the SnO_2 electrode modified with electrophoretically deposited layers of gold nanoclusters, the surface of which was covered with mixed SAMs of porphyrin-thiol and fullerene-thiol coupling molecules [100]. Li et al. also observed a photocurrent at a gold electrode modified with electrostatically deposited layers of gold nanoclusters, the surface of which

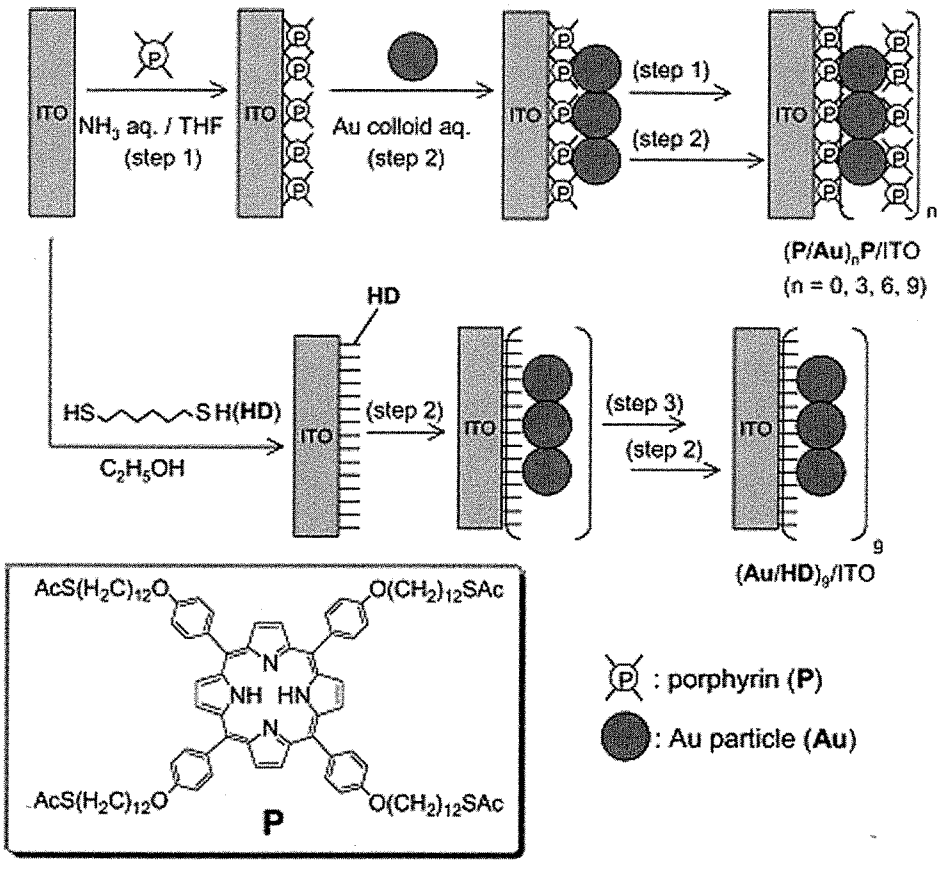

Figure 8. Schematic illustration for the fabrication of multilayer assemblies; $(\mathbf{P/Au})_n$P/ITO ($n = 0, 3, 6, 9$) and $(\mathbf{Au/HD})_9$/ITO. Reprinted with permission from [97], S. Yamada et al., *Thin Solid Films* 438–439, 70 (2003). © 2003, Elsevier.

was covered with a SAM of a porphyrin-viologen coupling molecule [101].

For a gold electrode modified with semiconductor nanocluster multilayers, a unique preparation procedure is employed. First, semiconductor nanoclusters that are covered with the surfactant sodium bis(2-ethylhexyl) sulfosuccinate (Aerosol OT, AOT) were prepared in reverse micelles [102]. Thereafter, dithiol SAMs were prepared on a gold surface, and then layers of the semiconductor nanoclusters were prepared by dipping the dithiol SAM-modified gold in a nanocluster dispersion (Fig. 9) [103–109]. It was confirmed by XPS that the terminated thiol group, which is not connected with the gold, in the dithiol SAMs on gold is covalently bonded to the surface atoms of the semiconductor nanoclusters [103] and, as a result, the SAM forms on the semiconductor nanocluster surface. Relatively large photocurrents were observed at gold electrodes modified with various kinds of semiconductor nanoclusters, such as CdS [104–107], ZnS [106], PbS [108], and CdSe [109], which were prepared by the above procedures shown in Figure 9. An interesting preparation method in which tellurium nanoclusters were electrochemically deposited on gold electrodes modified with SAMs of molecular templates, whose terminal

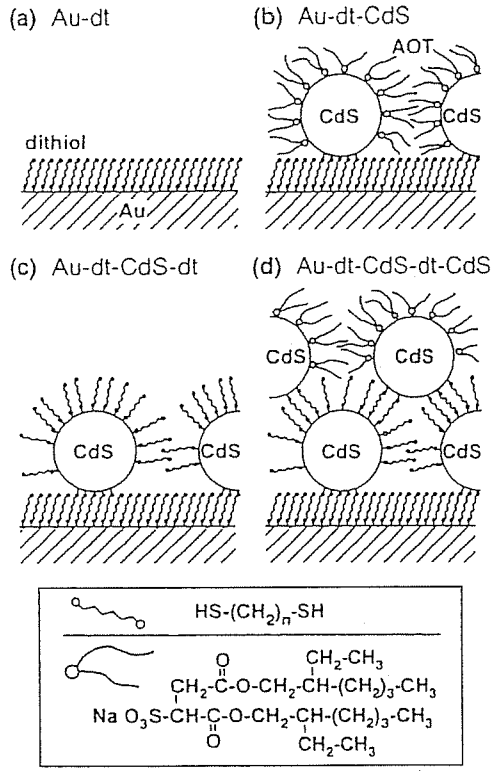

Figure 9. Schematic illustration of binding of CdS nanoclusters from reverse micelles onto gold via dithiol and the formation of an alternating layer-by-layer structure: (a) dithiol SAM on a gold substrate (Au-dt); (b) CdS nanoclusters attached on the SAM (Au-dt-CdS); (c) adsorption of dithiol layers on CdS nanoclusters (Au-dt-CdS-dt); (d) formation of a second CdS-nanocluster layer (Au-dt-CdS-dt-CdS). Each component is drawn in size according to the estimation from experimental results. Reprinted with permission from [103], T. Nakanishi et al., *J. Phys. Chem. B* 102, 1571 (1998). © 1998, American Chemical Society.

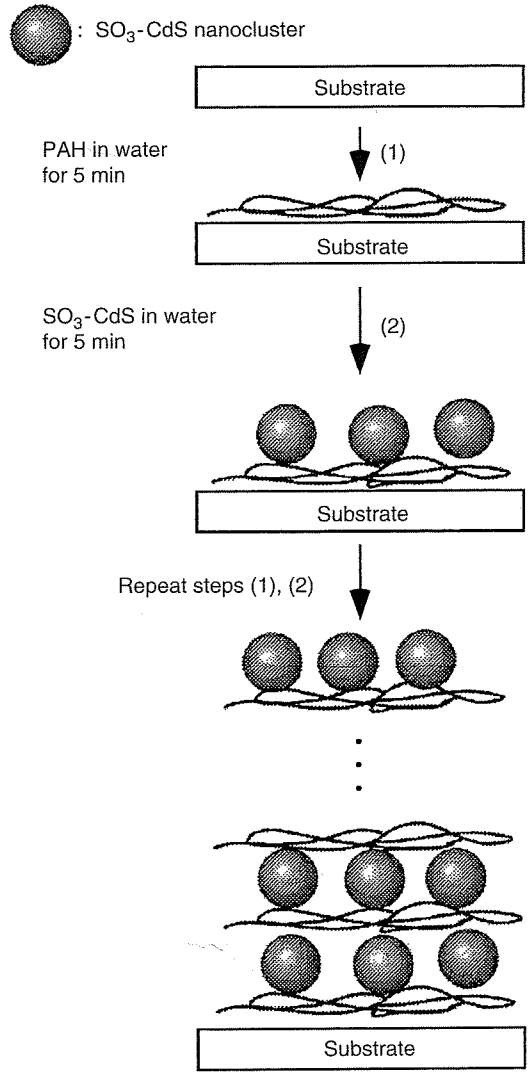

Figure 10. Procedures for preparing CdS nanoclusters/PAH multilayers by alternate two-step dip of the substrate into aqueous solutions containing CdS nanoclusters and PAH. Reprinted with permission from [112], K. Uosaki et al., *Faraday Discuss.* 125, 39 (2003). © 2003, Royal Society of Chemistry.

group is β-cyclodextrin (β-CD), has been reported [110]. Woo et al. observed a photocurrent at this SAM.

Another method has also been employed to construct multilayers of alkylthiol SAM-covered nanoclusters on the electrode surface [27–30, 111, 112]. Multilayers of semiconductor nanoclusters covered with alkylthiol SAMs, whose terminated groups are the charged groups, can be constructed on the basis of an electrostatic interaction (Fig. 10) [112]. Relatively large and stable photocurrents were observed at this electrode, and photoelectrochemical properties of the semiconductor nanoclusters were discussed on the basis of the quantum size effect [110, 111].

5. CONTROL OF ELECTRON TRANSFER BY PHOTOISOMERIZATION AT SAMs

We can control electron transfer using structure change of several functional groups immobilized in SAMs by their

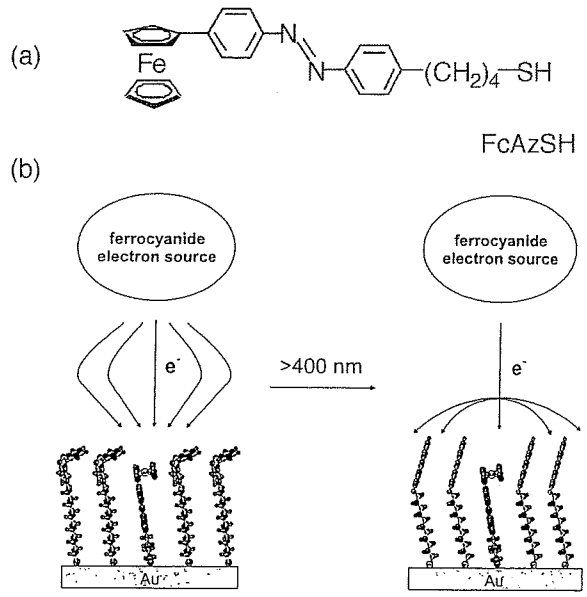

Figure 11. (a) FcAzSH molecule. (b) Schematic illustration of the control of electron transfer by photo-irradiation at FcAzSH SAM-modified gold electrodes. Reprinted with permission from [113], D. G. Walter et al., *J. Phys. Chem. B* 103, 402 (1999). © 1999, American Chemical Society.

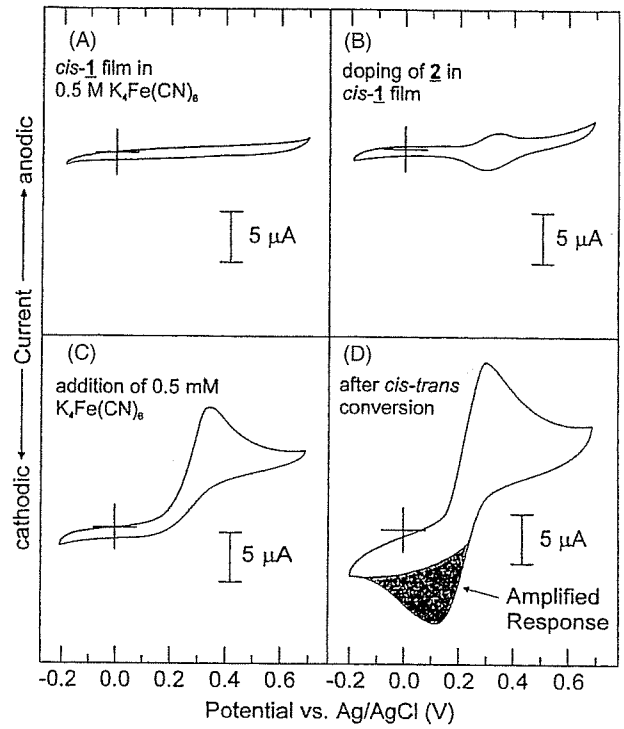

Figure 12. CVs for (a) a pure *cis*-AzSH SAM in the absence of light and in the presence of 0.5 mM $K_4Fe(CN)_6$, (b) *cis*-AzSH SAM after doping it with 1% FcAzSH (no $K_4Fe(CN)_6$), (c) two-component SAM (1:99 = FcAzSH:*cis*-azobenzenethiol) after addition of 0.5 mM $K_4Fe(CN)_6$ to the cell, and (d) two-component SAM, in the presence of 0.5 mM $K_4Fe(CN)_6$, after irradiation with >400 nm light for 1 h. The geometric area of the working electrode was 0.21 cm^2. The electrolyte used in all of the above experiments was 0.2 M $NaClO_4$. Scan rate = 100 $mV\,s^{-1}$. Reprinted with permission from [113], D. G. Walter et al., *J. Phys. Chem. B* 103, 402 (1999). © 1999, American Chemical Society.

photoisomerization; in other words, we can construct photoswitching systems using the photoisomerization property of SAMs.

Azobenzene is one of the most popular groups to photoisomerize with a structural change and has often been used even for alkylthiol SAMs [113–125]. Introduction of this group into SAMs enables construction of a photoswitching system. Mirkin et al. synthesized the ferrocene-azobenzene-thiol linked molecule (FcAzSH) shown in Figure 11(a) and achieved a photon-gated electron transfer at a gold electrode modified with mixed SAMs of FcAzSH and an azobenzene-thiol linked molecule (Fig. 11(b)) [113]. The electron source of this photon-gated electron transfer is ferrocyanide in the electrolyte solution. Figure 12(a) shows the CV of a gold electrode modified with a SAM of a *cis*-azobenzene-thiol molecule (*cis*-AzSH). For the *cis*-form SAM, no peaks due to the redox of ferrocyanide in the solution were observed. After doping of FcAzSH in the *cis*-form SAM, only redox peaks due to ferrocene fixed in the mixed SAM were observed (Fig. 12(b)). It should be noted that no redox species such as ferrocyanide were contained in this case. After the addition of ferrocyanide to the solution, however, a catalytic current due to the oxidation of ferrocyanide was observed (Fig. 12(c)) around the redox potential of ferrocene, showing that ferrocene fixed in this mixed SAM plays the role of a catalyst. After photoirradiation, reversible peaks due to the redox of both ferrocene fixed in this mixed SAM and ferrocyanide in the solution were observed (Fig. 12(d)). These electrochemical and photoelectrochemical behaviors showed that they achieved a photon-gated electron transfer.

Fujishima et al. found interesting electrochemical properties at a gold electrode modified with a SAM of azobenzene-thiol linked molecules [116–118] and with LB films of azobenzene derivatives [126–130]. The reduction potential of *cis*-azobenzene to hydrazobenzene is much more positive than that of the *trans* form. They also showed that reduced hydrazobenzene is electrochemically oxidized only to *trans*-azobenzene around +200 mV (vs. Ag/AgCl), even if the original form is the *cis* form. Using this phenomenon, we can control the charge-transfer rate at a gold electrode modified with a SAM of the azobenzene-ferrocene-thiol linked molecule (AzFcSH) shown in Figure 13(a) [119]. In a CV of a gold electrode modified with a SAM of 100% *trans*-form AzFcSH (Fig. 13(b)), only a pair of waves due to the redox of ferrocene in the potential range between 0 and +750 mV appeared and did not change shape after a potential scan or UV irradiation. The CV of gold modified with a SAM of 20% *cis*- and 80% *trans*-form AzFcSH (Fig. 13(c)), which was prepared from a solution containing AzFcSH after UV irradiation, also showed that only redox peaks due to ferrocene were observed in the potential range between +200 and +750 mV. When the potential was scanned to 0 mV, a pair of waves due to the redox of the azobenzene moiety appeared, in addition to that of ferrocene in the first potential scan (solid line in Fig. 13(d)). The wave due to the redox of azobenzene, however, disappeared, and the redox potential and the peak separation

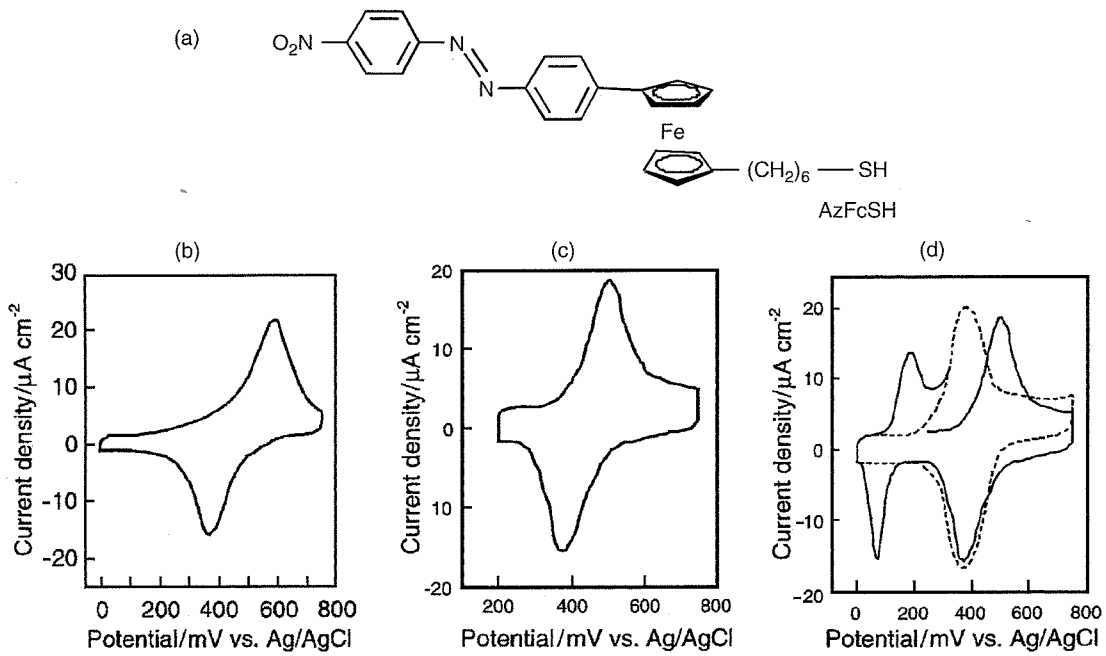

Figure 13. (a) AzFcSH molecule. CVs of (b) a 100% *trans*-AzFcSH SAM-modified gold electrode measured in the potential range between 0 and +750 mV and (c) a 20% *cis*- and 80% *trans*-AzFcSH SAM-modified gold electrode measured in the potential range between +200 and +750 mV. (d) The first scan (solid line) and second scan (dotted line) of the CVs of the 20% *cis*- and 80% *trans*-AzFcSH SAM-modified gold electrode measured in the potential region between 0 and +750 mV. Note that the potential scan was started from +200 mV in the positive direction. The electrolyte and scan rate in all of the above experiments were 0.1 M $HClO_4$ and 50 mV s^{-1}, respectively. Reprinted with permission from [119], T. Kondo et al., *Langmuir* 17, 6317 (2001). © 2001, American Chemical Society.

of the redox wave due to ferrocene became more negative and smaller, respectively, in the second scan (dotted line in Fig. 13(d)). The redox potential and the peak separation returned to the original values after UV irradiation. These changes in the electrochemical characteristics of the latter electrode were reversible. On the basis of the results of structural analysis by *in-situ* Fourier-transform infrared reflection absorption spectroscopy (FT-IRRAS), we concluded that the electrochemical properties, that is, the redox potential and the charge transfer rate, of the ferrocene group in the SAM can be reversibly controlled by electro- and photochemical structural conversions between the *cis* and *trans* forms of the azobenzene moiety in the SAM (Fig. 14).

Spiropyran/merocyanine photoisomerization was also used at alkylthiol SAMs to gate/ungate electron transfer [131–134]. Willner et al. constructed a spiropyran/merocyanine-terminated SAM-modified gold electrode using synthesized β-1-[3,3-dimethyl-6′-nitrospiro(indoline-2,2′-2*H*-benzopyran)] propionic acid and an amine-terminated alkylthiol SAM (Fig. 15). Using this SAM, they achieved photo-switchable on/off bioactivities. Figure 16 shows an example of their photoswitchable on/off bioactivity systems (redox of cytochrome *c*) using this SAM-modified electrode [131, 132]. In this case, they used a mixed SAM of spiropyran/merocyanine-terminated and 4-pyridine thiol.

In addition to photoisomerization of the azobenzene and spiropyran/merocyanine system, (pyridylazo)benzene [135], stilbene [136], and diarylethene [137] were used as photoisomerization groups in alkylthiol SAM-modified electrodes.

Matsui et al. successfully controlled molecular recognition by photoisomerization of an azobenzene group [138]. They used peptide nanotubes, which were self-assembled from peptide bolaamphiphile, as templates to fabricate azobenzene nanotubes. This peptide nanotube incorporates amide sites to anchor decorating molecules such as proteins, nanocrystals, and porphyrins via hydrogen bonding. To anchor the azobenzene nanotubes onto surfaces, a SAM of thiolated α-cyclodextrins (α-CD) molecules was used on the patterned Au substrates, the preparation method of which is described in Section 7 (Fig. 17).

6. LUMINESCENCE FROM SAMs

Luminescence from photoactive SAMs has been extensively studied. Fox and Wooten constructed a SAM of anthracene-thiol linked molecules, measured the luminescent intensity and FT-IR spectrum of the SAMs, and investigated dimer formation of the anthracene moiety in this SAM [139]. Guo et al. constructed a photoactive and electrochemical active myoglobin protein layer on gold surfaces modified with SAMs of metalloporphyrin-thiol linked molecules by reconstitution of apomyoglobin in solution with the corresponding metalloporphyrin and investigated their fluorescence spectra [140]. Fluorescence from mixed SAMs of the ferrocene-thiol derivative and Zn tetraarylporphyrin-thiol derivative were measured under open circuit conditions, and the amounts of the photostoraged charge in the SAM were quantitatively examined by Roth and co-workers [141]. Bohn et al. constructed protein-connected SAMs by using the procedures

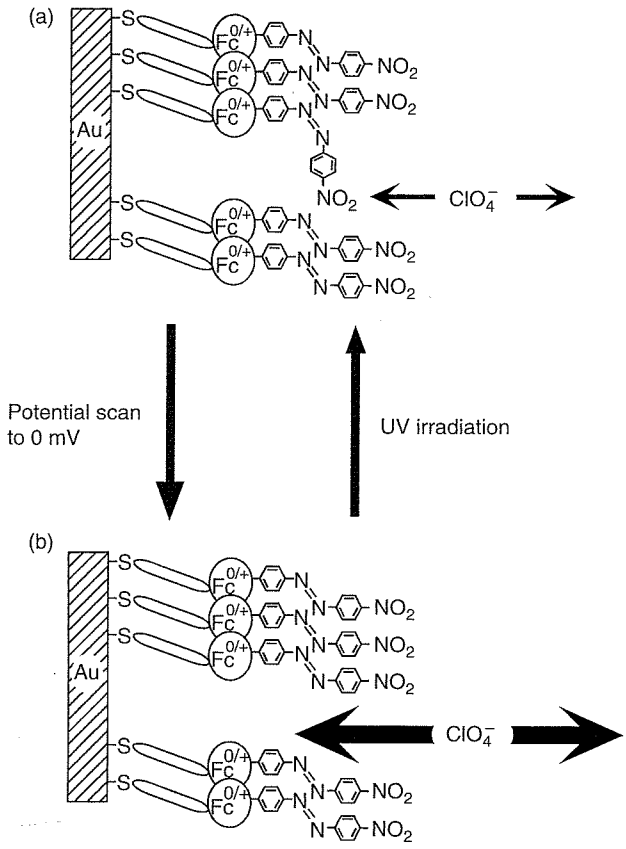

Figure 14. Schematic illustration at the interface (a) between a 100% *trans*-AzFcSH SAM-modified gold electrode and electrolyte solution containing perchlorate anions and (b) between a 20% *cis*- and 80% *trans*-AzFcSH SAM-modified gold electrode and electrolyte solution containing perchlorate anions before the potential scan to 0 mV. Reprinted with permission from [119], T. Kondo et al., *Langmuir* 17, 6317 (2001). © 2001, American Chemical Society.

shown in Figure 18, measured the fluorescence intensity from a polystyrene nanosphere doped as a fluorescent label in the SAMs, and investigated cellular adhesion and motility by measuring the surface composition gradients of extracellular matrix proteins such as fibronectin [142, 143].

Electrochemical and electrogenerated chemiluminescence (ECL) from gold and ITO electrodes modified with a SAM of tris(2,2′-bipyridine)ruthenium(II) ($Ru(bpy)_3^{2+}$)-thiol linked molecules (Fig. 19(a) [144]) have been reported. The potential dependence of the emission intensity (Fig. 19(b-b)) and luminescent spectrum (Fig. 20) were observed at a $Ru(bpy)_3^{2+}$ SAM-modified electrode in a solution containing $C_2O_4^{2-}$, and the following reactions were considered to take place within the positive potential region where emission was observed [144]:

$$Ru(bpy)_3^{2+} \rightarrow Ru(bpy)_3^{3+} + e^- \quad (1)$$

$$Ru(bpy)_3^{3+} + C_2O_4^{2-} \rightarrow Ru(bpy)_3^{2+} + CO_2 + CO_2^{\bullet -} \quad (2)$$

$$Ru(bpy)_3^{3+} + CO_2^{\bullet -} \rightarrow Ru(bpy)_3^{2+*} + CO_2 \quad (3)$$

$$Ru(bpy)_3^{2+*} \rightarrow Ru(bpy)_3^{2+} + h\nu \quad (4)$$

$$Ru(bpy)_3^{2+*} \rightarrow Ru(bpy)_3^{3+} + e^- \quad (5)$$

In these processes, electrochemically generated $Ru(bpy)_3^{3+}$ oxidizes $C_2O_4^{2-}$, forming CO_2 and $CO_2^{\bullet -}$, and becomes $Ru(bpy)_3^{2+}$, which again donates an electron to the electrode (reaction (1)). Thus, the $Ru(bpy)_3^{2+/3+}$ head group in the SAM acts as a mediator for the oxidation of oxalate, and therefore, a monotonic increase in the anodic current was observed as the potential became more positive (Fig. 19(b-a)). $CO_2^{\bullet -}$ reduces $Ru(bpy)_3^{3+}$ to $Ru(bpy)_3^{2+*}$, which has excess energy. $Ru(bpy)_3^{2+*}$ may directly donate an electron to the electrode (reaction (5)) or relax to $Ru(bpy)_3^{2+}$ with light emission efficiency controlled by the electron transfer rate of reaction (5), which should be dependent on

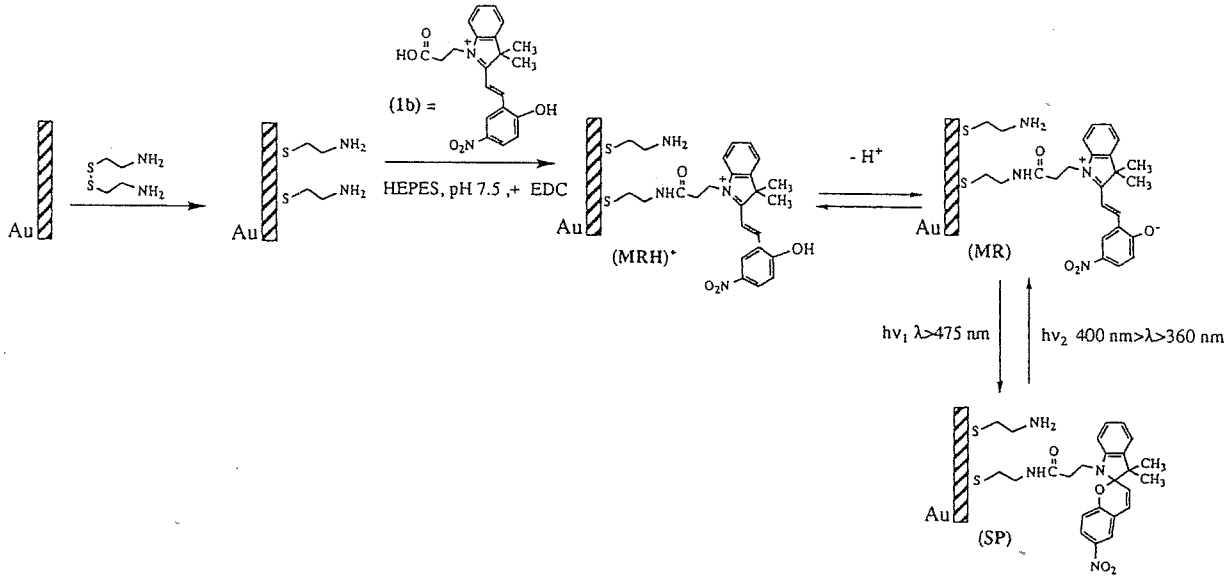

Figure 15. Schematic modification procedure of a gold electrode by a photoisomerizable spyropyran SAM. Reprinted with permission from [132], E. Katz et al., *J. Electroanal. Chem.* 382, 25 (1995). © 1995, Elsevier.

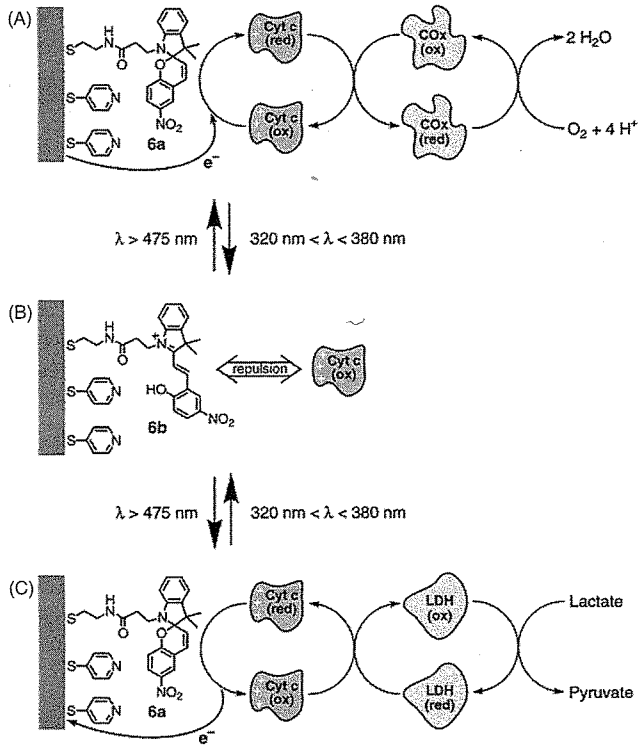

Figure 16. Schematic coupling model of the photoswitchable interactions between cytochrome *c* and mixed SAM of spiropyran/merocyanine-terminated and 4-pyridinethiol with (a) reduction of O_2 by CO_x and (c) oxidation of lactate by lactate dehydrogenase (LDH). (b) When the electrode is in the cationic merocyanine state, repulsive interactions disallow functioning of the bioelectrocatalytic processes. Reprinted with permission from [131], A. N. Shipway and I. Willner, *Acc. Chem. Res.* 34, 421 (2001). © 2001, American Chemical Society.

the distance between the electrode and the $Ru(bpy)_3^{2+/3+}$ head group in the SAM. Bard et al. also used the following oxidation reaction of tripropylamine (TPrA) and the above reactions (1 and 4), and they observed ECL from the

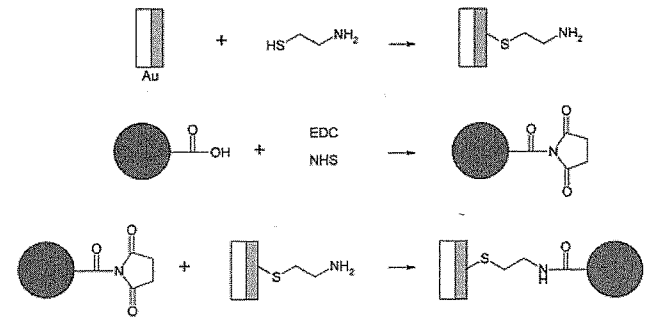

Figure 18. Schematic modification process of fluorescent nanospheres containing a large number (~10^6 per sphere) of pendant carboxylic acid moieties, which were exploited to couple the nanospheres to amine-terminated thiol SAMs through amide bond formation. Reprinted with permission from [142], S. T. Plummer and P. W. Bohn, *Langmuir* 18, 4142 (2002). © 2002, American Chemical Society.

generated $Ru(bpy)_3^{2+*}$ at SAM-modified gold and platinum electrodes [147, 148].

$$TPrA \rightarrow TPrA^{\bullet+} + e^- \quad (6)$$

$$Ru(bpy)_3^{3+} + TPrA \rightarrow Ru(bpy)_3^{2+} + TPrA^{\bullet+} \quad (7)$$

$$TPrA^{\bullet+} \rightarrow TPrA^{\bullet} + H^+ \quad (8)$$

$$Ru(bpy)_3^{3+} + TPrA^{\bullet} \rightarrow Ru(bpy)_3^{2+*} + \text{products} \quad (9)$$

Using this ECL behavior of the $Ru(bpy)_3^{2+}$/TPrA system, the surface hydrophobicity [147] and immobilization of DNA and protein [148] were investigated. Except for in the above-described studies, ECL behaviors at the $Ru(bpy)_3^{2+}$ SAM-modified electrodes were used to fabricate an opto-electrochemical microring array [149].

The application of a SAM in an electroluminescence (EL) device has been reported (Fig. 21 shows a schematic drawing of EL process). Yamashita et al. used gold electrodes modified with SAMs of tripod-shaped π-conjugated thiols and disulfide (Figs. 22(a–c)) and

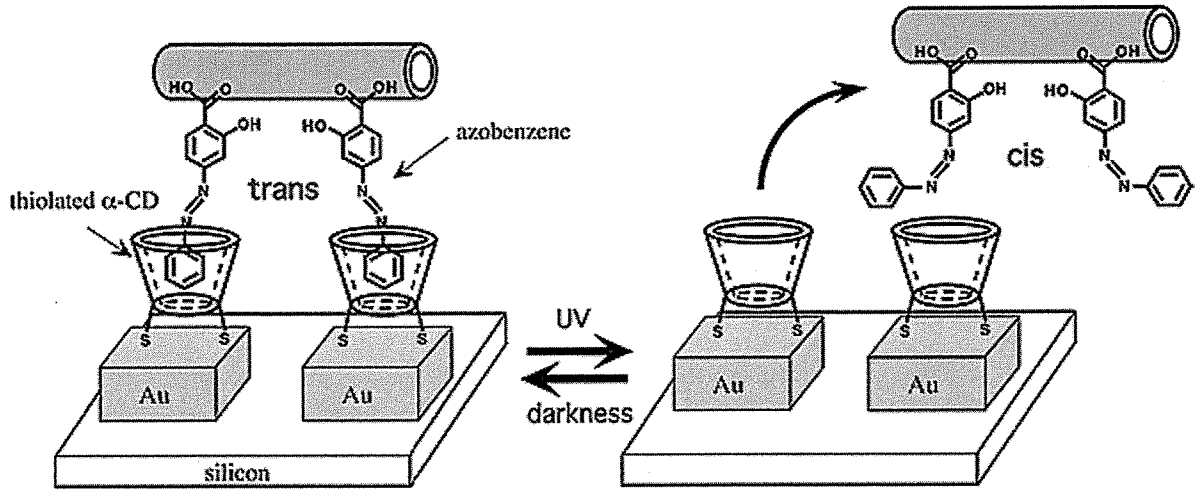

Figure 17. Schematic diagram of an azobenzene nanotube assembly on complementary α-CD SAM/Au substrates via host–guest molecular recognition and light-induced nanotube detachment/attachment on the α-CD SAM surface. Reprinted with permission from [138], I. A. Banerjee et al., *J. Am. Chem. Soc.* 125, 9542 (2003). © 2003, American Chemical Society.

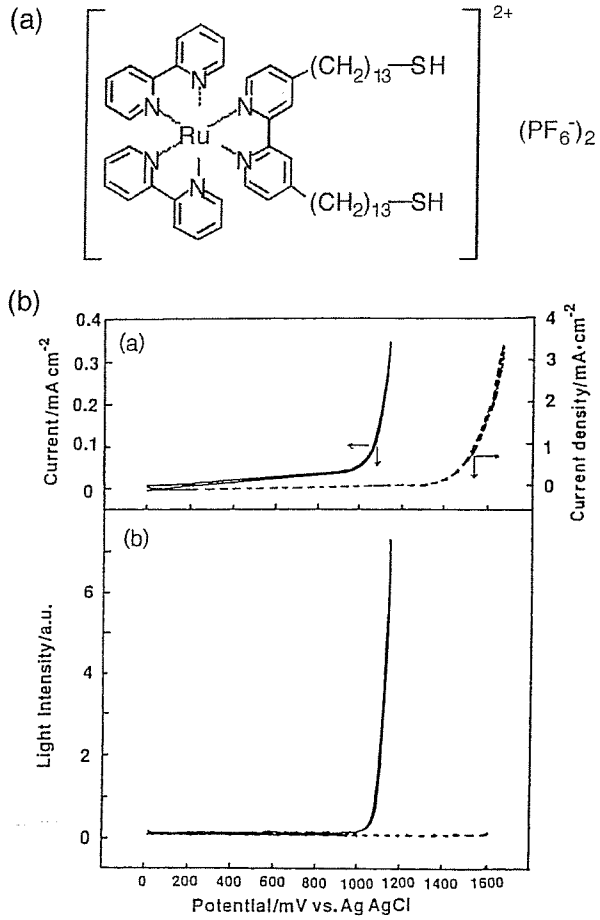

Figure 19. (a) tris(2,2′-Bipyridine)ruthenium(II) ($Ru(bpy)_3^{2+}$)-thiol linked molecule. Potential dependence of (b) currents of the unmodified (broken curve) and SAM-modified (solid curve) ITO electrodes, and (c) ECL intensity of the unmodified (broken curve) and SAM-modified (solid curve) ITO electrodes in a solution containing 0.4 M Na_2SO_4 + 0.1 M $Na_2C_2O_4$. Reprinted with permission from [144], Y. Sato and K. Uosaki, *J. Electroanal. Chem.* 384, 57 (1995). © 1995, Elsevier.

investigated enhanced hole injection from the EL of these SAM-modified electrodes [150]. They constructed layers of 4,4″-bis(3-methylphenyl-phenylamino)biphenyl (TPD), tris(8-hydroxyquinolinato)aluminum(III) (Alq_3) and Mg-Ag alloy as hole transport, emission, and electron transport layers, respectively, on these SAMs by vacuum evaporation. As a reference, these layers deposited both on bare gold and bare ITO substrates were also used. Figures 22(d) and (e) show the EL characteristics of these devices. Both the current-voltage (*I-V*) and luminescence-voltage (*L-V*) curves of these devices shifted to higher voltages in the order of SAM(b) < SAM(a) ~ bare ITO < bare gold < SAM(c), where SAM(a), SAM(b) and SAM(c) represent the SAM of the molecules (a), (b) and (c), respectively, shown in Figure 22. Compared to the bare gold device, the SAM(b) device exhibited significantly improved EL performance, for example, greatly reduced operating potential, yielding much greater maximum brightness and permitting much higher current and better stability. In contrast, the SAM(c) device showed EL characteristics poorer than those of the bare gold

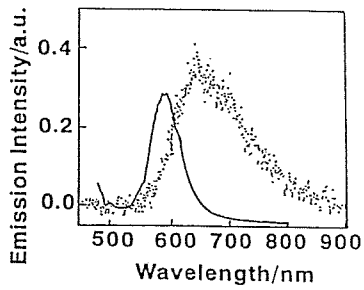

Figure 20. ECL spectrum of a $Ru(bpy)_3^{2+}$-thiol SAM-modified ITO electrode in a solution containing 0.4 M Na_2SO_4 + 0.1 M $Na_2C_2O_4$ at 1.15 V (dots) and the emission spectrum of $Ru(bpy)_3^{2+}$-thiol in CH_2Cl_2 solution (solid curve). Reprinted with permission from [144], Y. Sato and K. Uosaki, *J. Electroanal. Chem.* 384, 57 (1995). © 1995, Elsevier.

device. The different effects of the SAMs on EL properties of the devices were concluded to be due to the modification density of the SAMs, leading to a vacuum-level shift at the Au/TPD interface by the SAMs. The results of CVs at the gold electrodes modified with these SAMs showed that the packing of the tripod-shaped thiol SAM(b) was compact, that of the thiol SAM(a) was less compact, and that of the disulfide SAM(c) was very poor. These modifications influence the hole injection barrier height at the Au/TPD interface and then affect the EL characteristics of the devices.

It is quite important to apply a photoactive SAM to a biosensor, detecting the fluorescence from it [151, 152]. Sato et al. investigated the electro-oxidative chemiluminescence from a luminol/hydrogen peroxide system catalyzed by a ferrocene-thiol SAM-modified gold electrode (Fig. 23). When luminol and hydrogen peroxide were contained in the electrolyte solution, in addition to an oxidation peak due to the redox of ferrocene, a catalytic oxidation current of luminol was observed (solid line in Fig. 23(a)) and light emission was simultaneously observed (open circles in Fig. 23(b)). The ECL intensity depended on the pH of the solution. They used this system for detecting glucose in the presence of glucose oxidase [152].

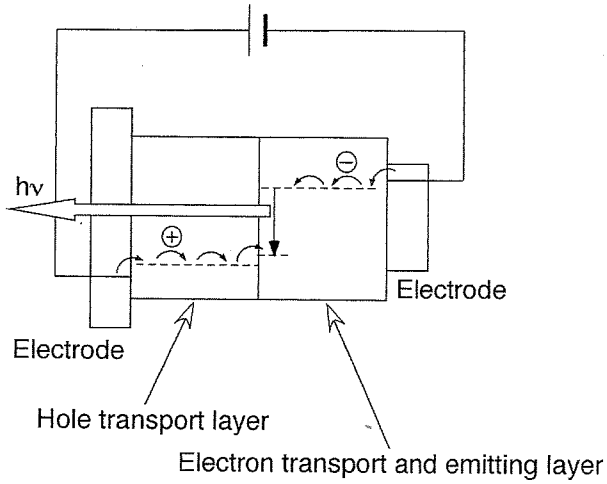

Figure 21. Schematic drawing of EL process.

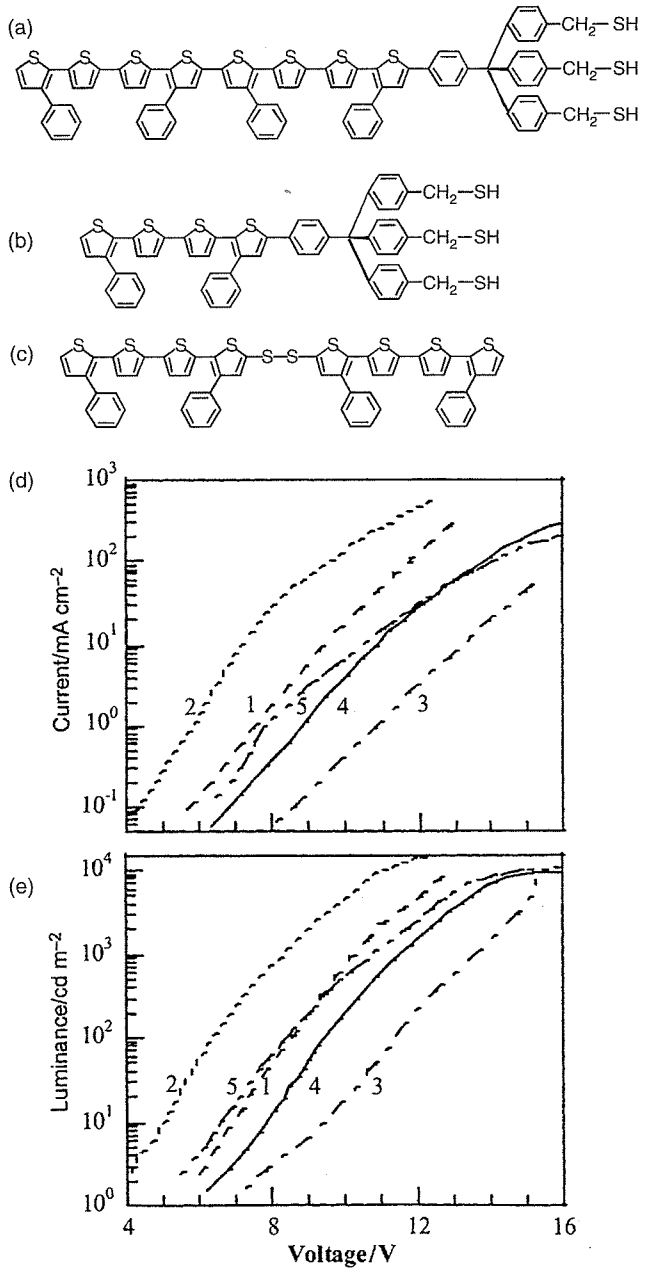

Figure 22. (a), (b) Tripod-shaped π-conjugated thiol and (c) π-conjugated disulfide molecules. (d) *I-V* and (e) *L-V* characteristics of (1) SAM(a), (2) SAM(b), (3) SAM(c), (4) bare gold, and (5) bare ITO devices. Reprinted with permission from [150], L. Zhu et al., *J. Mater. Chem.* 12, 2250 (2002). © 2002, Royal Society of Chemistry.

There is an interesting report about fluorescence from a porphyrin incorporated in a SAM. Reich et al. constructed Au and Au/Ni nanowires whose surfaces were modified with SAMs of porphyrin-thiol coupling molecules [153]. Fluorescence microscopy was used to optimize the functionalization of two-segment gold–nickel nanowires for selectivity and stability of the nanowire–molecule linkages. Magnetic trapping was employed as a technique in which single nanowires are captured from a fluid suspension using lithographically patterned micromagnets. They investigated the influence of an external magnetic field on this process and suggested a

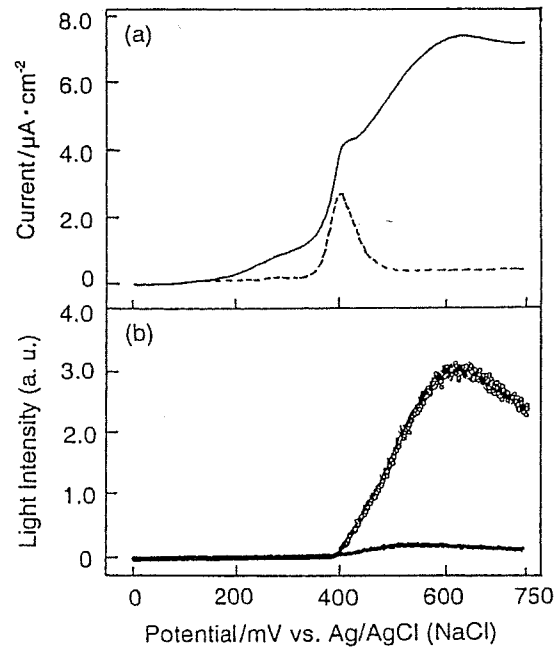

Figure 23. (a) Linear sweep voltammograms of a ferrocene-thiol SAM-modified gold electrode measured in electrolyte solution (0.1 M $NaClO_4$/0.1 M buffer solution, pH 8.2) with 100 μM luminol and 10 mM H_2O_2 (solid line) and without luminol and H_2O_2 (dotted line). Sweep rate: 2 mV s^{-1}. (b) ECL intensities of a ferrocene-thiol SAM-modified gold electrode (open circles) simultaneously measured with the linear sweep voltammograms. ECL intensity of unmodified gold electrode (closed diamonds). Reprinted with permission from [151], Y. Sato et al., *Chem. Lett.* 1330 (2000). © 2000, Chemical Society of Japan.

model based on the interplay of dipolar forces and viscous drag from the results of investigation of the dynamics of the magnetic trapping.

7. PHOTOPATTERNING USING SAMs

As modern technology proceeds every year, the required resolution of patterning becomes much higher. Since Whitesides published a concept of microcontact printing using SAMs of alkylsiloxanes [154, 155], many studies on photopatterning using SAMs of alkylthiols have been carried out [156–167] because the use of alkylthiol SAMs with a high packing density leads to patterning with a high spatial resolution.

Crooks et al. reported patterning with a high resolution employing the following procedures shown in Figure 24(a) [157]. At first, they placed the transmission electron microscope (TEM) minigrid as a photomask in contact with a SAM composed of closed-packed HOOC-$(CH_2)_{10}$-C≡C—C≡C-$(CH_2)_{10}$-SH confined to a Au/Cr/Si surface (Fig. 24(a-A)). The entire assembly is then exposed to UV light, which induces polymerization in the unmasked regions of the SAM (Fig. 24(a-B)). Next, the unpolymerized portion of the resist is selectively desorbed using an electrochemical reductive stripping method [43] (Fig. 24(a-C)). Selective stripping is possible because the polymeric SAM is sufficiently insoluble and strongly bound to the surface through multiple Au/S and van der Waals interactions, so

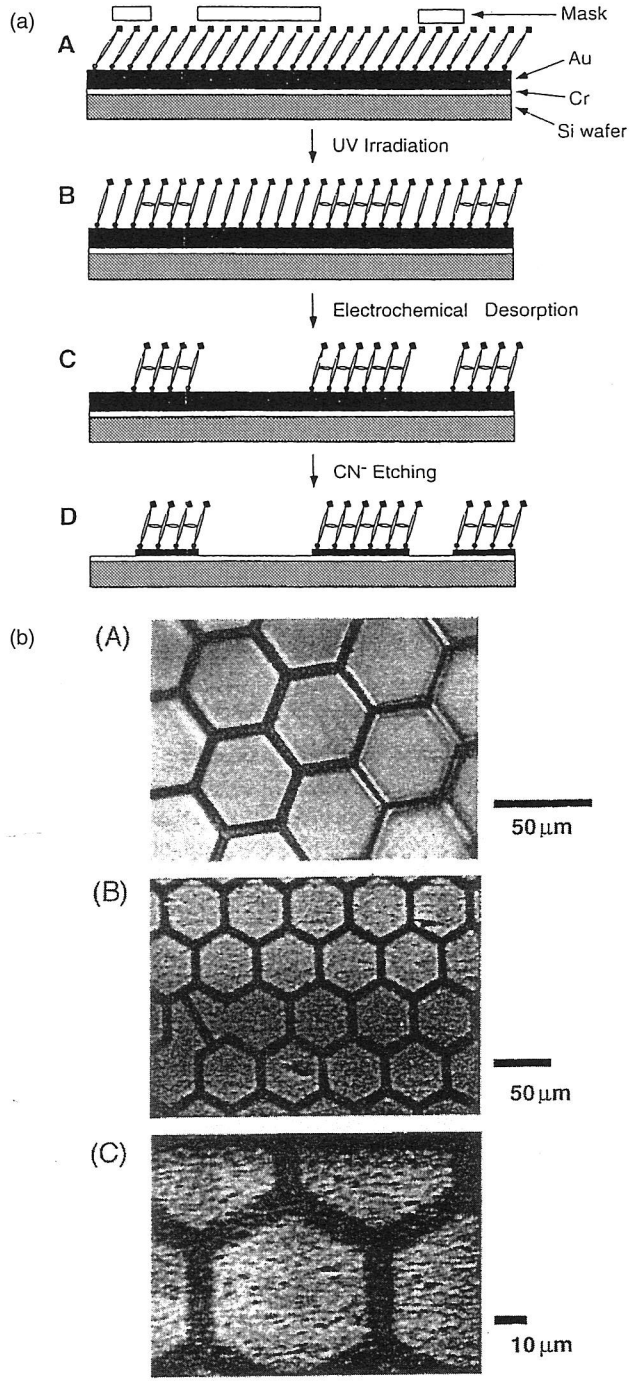

Figure 24. (a) Schematic illustration of the process for making a photopatterned surface using an $HOOC(CH_2)_{10}C{\equiv}C{-}C{\equiv}C(CH_2)_{10}SH$ molecule. (b) (A) Optical micrograph of the 400-mesh minigrid used to generate the patterns shown in (B and C). Note that the right and left sides of this micrograph are slightly out of focus. (B, C) Scanning electron micrographs of a Au surface patterned using the 400-mesh TEM minigrid shown in (A). Reprinted with permission from [157], K. C. Chan et al., *J. Am. Chem. Soc.* 117, 5875 (1995). © 1995, American Chemical Society.

that it survives potential excursions that remove monomeric alkylthiol SAMs. Resist removal results in a negative image of the mask, which can be elaborated by etching the grid image into the Au surface with an O_2-saturated 1 M KOH + 10 mM KCN aqueous solution (Fig. 24(a-D)). Figure 24(b-A) is an optical micrograph of a 400-mesh (holes per linear inch) Cu TEM minigrid, which was used to pattern the Au surface. Figures 24(b-B) and 24(b-C) are scanning electron micrographs (SEMs) of a patterned Au surface, such as that illustrated in Figure 24(a-D) obtained at two different magnifications. At this level of resolution, they observed excellent reproduction of the mask features. However, close inspection reveals that the lateral dimensions of the hexagonal raised regions are somewhat less than those of the original mask. This may arise from diffraction off the mask edges, that is, from the modulation transfer function, which will tend to reduce the photon flux in areas near the vicinity of the mask edges.

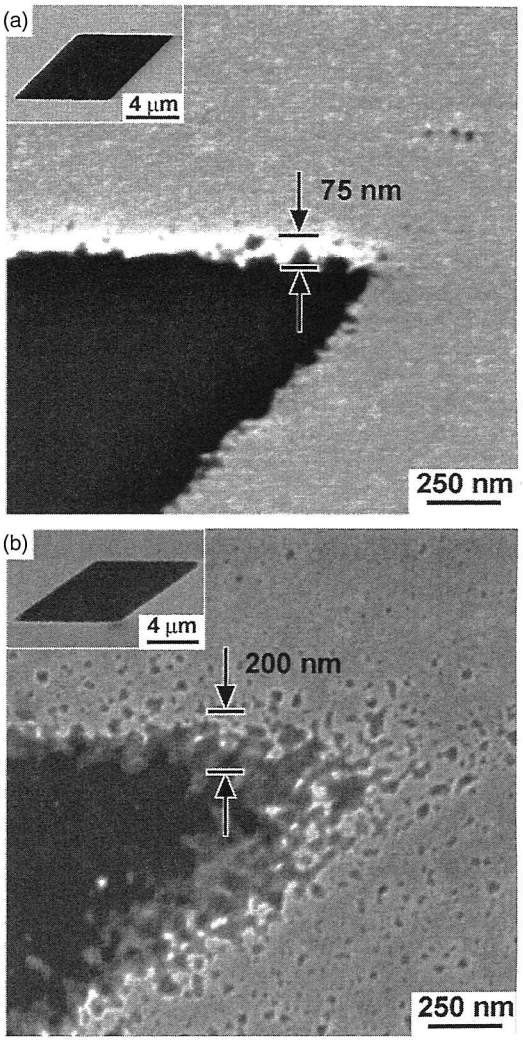

Figure 25. (a) SEM of a diamond pattern on Pd. The pattern was generated by two consecutive printings of 5-μm lines (10-μm pitch) at an angle of ~30° relative to one another. The edge roughness is ~30–70 nm and the radius of curvature at the point of the structure is ~40–50 nm. The inset shows the whole diamond. (b) SEM of a diamond pattern of gold. Note the increase in the number of pits in the surface of the gold and the radius of curvature in the point (~150 nm). Reprinted with permission from [161], J. C. Love et al., *J. Am. Chem. Soc.* 124, 1576 (2002), © 2002, American Chemical Society.

Legget et al. developed a scanning near-field photolithography technique in which a near-field scanning optical microscope (NSOM) coupled to a UV laser is used to selectively oxidize alkylthiols in SAMs [166, 167]. The weakly bound alkylthiolate oxidation products may either be replaced by contrasting alkylthiols to yield patterned structures as small as 20 nm or be used as resist for the etching of three-dimensional structures into the underlying substrate. They used this technique not only to make photopatterning but also to investigate the kinetics of SAM photo-oxidation.

Generally, an alkylthiol SAM on gold leaves defects and surface pits during etching, as described in detail in Section 6, and an alkylthiol SAM on gold as a substrate is therefore not useful for construction of a patterned surface without any defects. Whitesides et al. used palladium as a substrate material to construct a patterned surface without defects [161]. Figure 25 shows structures that they can generate by the combination of microcontact printing and etching on palladium and on gold. Both films were patterned with hexadecanethiol and exposed to the most selective etchants. As clearly seen, structures on the palladium film show better edge definition and 85–90% fewer etch pits on the surface than on the gold film (particularly near the edges of the structures).

8. CONCLUSIONS

There have been studies on photocharacteristics using alkylthiol SAMs on metals because the molecules in SAMs are arranged in order at the molecular level. Thus, we cannot review all of the related papers here. As examples, there are nonlinear optical properties [169–171], surface plasmon [172, 173], single-molecule spectroscopy [174], and so on. We expect that photoactive SAMs will be extensively investigated in a wide variety of scientific fields and will play increasingly important roles in modern nanotechnology.

REFERENCES

1. J. Sagiv, *J. Am. Chem. Soc.* 102, 92 (1980).
2. A. Ulman, "An Introduction to Ultrathin Organic Films from Langmuir-Blodgett to Self-Assembly." Academic Press, New York, 1991.
3. H. O. Finklea, "Electroanalytical Chemistry" (A. J. Bard and I. Rubinstein, Eds.), Vol. 19, pp. 109–335. Marcel Dekker, New York, 1996.
4. K. Uosaki, "New Challenges in Organic Electrochemistry" (T. Osa, Ed.), pp. 99–111. Gordon and Breach, Amsterdam, 1998.
5. A. Ulman, *Chem. Rev.* 96, 1533 (1996).
6. R. Yamada and K. Uosaki, *Langmuir* 13, 5218 (1997).
7. R. Yamada and K. Uosaki, *Langmuir* 14, 855 (1998).
8. S. Xu, S. J. N. Cruchon-Dupeyrat, J. C. Garno, G.-Y. Liu, J. G. Kane, T.-H. Yong, and P. E. Laibinis, *J. Chem. Phys.* 108, 5002 (1998).
9. K. Uosaki, Y. Sato, and H. Kita, *Langmuir* 7, 1510 (1991).
10. K. Uosaki, Y. Sato, and H. Kita, *Electrochim. Acta* 36, 1799 (1991).
11. K. Shimazu, I. Yagi, Y. Sato, and K. Uosaki, *Langmuir* 8, 1385 (1992).
12. Y. Sato, H. Itoigawa, and K. Uosaki, *Bull. Chem. Soc. Jpn.* 66, 1032 (1993).
13. K. Shimazu, I. Yagi, Y. Sato, and K. Uosaki, *J. Electroanal. Chem.* 372, 117 (1994).
14. Y. Sato, B. L. Frey, R. M. Corn, and K. Uosaki, *Bull. Chem. Soc. Jpn.* 67, 21 (1994).
15. K. Shimazu, S. Ye, Y. Sato, and K. Uosaki, *J. Electroanal. Chem.* 375, 409 (1994).
16. T. Otsuka, Y. Sato, and K. Uosaki, *Langmuir* 10, 3658 (1994).
17. T. Kondo, M. Takechi, Y. Sato, and K. Uosaki, *J. Electroanal. Chem.* 381, 203 (1995).
18. S. Ye, Y. Sato, and K. Uosaki, *Langmuir* 13, 3157 (1997).
19. Y. Sato, M. Fujita, F. Mizutani, and K. Uosaki, *J. Electroanal. Chem.* 409, 145 (1996).
20. S. Ye, A. Yashiro, Y. Sato, and K. Uosaki, *J. Chem. Soc., Faraday Trans.* 92, 3813 (1996).
21. Y. Sato, S. Ye, T. Haba, and K. Uosaki, *Langmuir* 12, 2726 (1996).
22. M. Abe, T. Kondo, K. Uosaki, and Y. Sasaki, *J. Electroanal. Chem.* 473, 93 (1999).
23. M. Abe, A. Sato, T. Inomata, T. Kondo, K. Uosaki, and Y. Sasaki, *J. Chem. Soc., Dalton Trans.* 2693 (2000).
24. A. Sato, M. Abe, T. Inomata, T. Kondo, S. Ye, K. Uosaki, and Y. Sasaki, *Phys. Chem. Chem. Phys.* 3, 3420 (2001).
25. T. Kondo, M. Okamura, and K. Uosaki, *J. Organomet. Chem.* 637–639, 841 (2001).
26. T. Kondo, T. Sumi, and K. Uosaki, *J. Electroanal. Chem.* 538/539, 59 (2002).
27. T. Kondo, M. Okamura, and K. Uosaki, *Chem. Lett.* 930 (2001).
28. K. Uosaki, T. Kondo, M. Okamura, and W. Song, *Faraday Discuss.* 121, 373 (2002).
29. W. Song, M. Okamura, T. Kondo, and K. Uosaki, *J. Electroanal. Chem.* 554/555, 385 (2003).
30. S. Wenbo, M. Okamura, T. Kondo, and K. Uosaki, *Phys. Chem. Chem. Phys.* 5, 5279 (2003).
31. T. Sumi, H. Wano, and K. Uosaki, *J. Electroanal. Chem.* 550–551, 321 (2003).
32. H. Wano and K. Uosaki, *Langmuir* 17, 8224 (2001).
33. C. E. D. Chidsey and D. N. Loiacono, *Langmuir* 6, 682 (1990).
34. C. E. D. Chidsey, C. R. Bertozzi, T. M. Putvinski, and A. M. Mujsce, *J. Am. Chem. Soc.* 112, 4301 (1990).
35. L. De, C. Hugh, and D. A. Buttry, *Langmuir* 6, 1319 (1990).
36. C. Miller, P. Cuendet, and M. Grätzel, *J. Phys. Chem.* 95, 877 (1991).
37. J. J. Hickman, D. Ofer, C. Zou, M. S. Wrighton, P. E. Laibinis, and G. M. Whitesides, *J. Am. Chem. Soc.* 113, 1128 (1991).
38. C. E. D. Chidsey, *Science* 251, 919 (1991).
39. D. M. Collard and M. A. Fox, *Langmuir* 7, 1192 (1991).
40. S. L. Miehelhaugh, C. Bhardwaj, G. J. Cali, B. G. Bravo, M. E. Bothwell, G. M. Berry, and M. P. Soriaga, *Corrosion* 47, 322 (1991).
41. S. E. Creager and G. K. Rowe, *Anal. Chim. Acta* 246, 233 (1991).
42. D. Mandler and A. J. Bard, *J. Electroanal. Chem.* 307, 217 (1991).
43. C. A. Widrig, C. Chung, and M. D. Porter, *J. Electroanal. Chem.* 310, 335 (1991).
44. L. Sun and R. M. Crooks, *J. Electrochem. Soc.* 138, L23 (1991).
45. M. A. Bryant and J. E. Pemberton, *J. Am. Chem. Soc.* 113, 8284 (1991).
46. H. O. Finklea and D. D. Hanshew, *J. Am. Chem. Soc.* 114, 3173 (1992).
47. L. Stryer, "Biochemistry," 3rd Edition, Freeman, New York, 1988.
48. J. Deisenhofer, O. Epp, K. Miki, R. Huber, and H. Michel, *J. Mol. Biol.* 180, 385 (1984).
49. P. Seta, E. Bienvenue, A. L. Moore, P. Mathis, R. V. Bensasson, P. Liddell, P. J. Pessiki, A. Joy, and T. A. Moore, *Nature* 316, 653 (1985).
50. Y. Sakata, H. Tatemitsu, E. Bienvenue, and P. Seta, *Chem. Lett.* 1625 (1988).
51. M. Fujihira, *Mol. Cryst. Liq. Cryst.* 183, 59 (1990).
52. M. Fujihira, K. Nishiyama, and H. Yamada, *Thin Solid Films* 132, 77 (1985).
53. M. Fujihira and H. Yamada, *Thin Solid Films* 160, 125 (1988).
54. M. Sakomura and M. Fujihira, *Thin Solid Films* 243, 616 (1994).

55. M. Fujihira, M. Sakomura, D. Aoki, and A. Koike, *Thin Solid Films* 273, 168 (1996).
56. T. Kondo, T. Ito, S. Nomura, and K. Uosaki, *Thin Solid Films* 284/285, 652 (1996).
57. T. Kondo, M. Yanagida, S. Nomura, T. Ito, and K. Uosaki, *J. Electroanal. Chem.* 438, 121 (1997).
58. K. Uosaki, T. Kondo, X.-Q. Zhang, and M. Yanagida, *J. Am. Chem. Soc.* 119, 8367 (1997).
59. M. Yanagida, T. Kanai, X.-Q. Zhang, T. Kondo, and K. Uosaki, *Bull. Chem. Soc. Jpn.* 71, 2555 (1998).
60. T. Kondo, T. Kanai, K. Iso-o, and K. Uosaki, *Z. Phys. Chem.* 212, 23 (1991).
61. T. Kondo, M. Yanagida, X.-Q. Zhang, and K. Uosaki, *Chem. Lett.* 964 (2000).
62. H. Imahori, H. Yamada, Y. Nishimura, I. Yamazaki, and Y. Sakata, *J. Phys. Chem.* 104, 2009 (2000).
63. H. Imahori, H. Norieda, S. Ozawa, K. Ushida, H. Yamada, T. Azuma, K. Tamaki, and Y. Sakata, *Langmuir* 14, 5335 (1998).
64. H. Imahori, H. Yamada, S. Ozawa, K. Ushida, and Y. Sakata, *Chem. Commun.* 1165 (1999).
65. H. Imahori, T. Azuma, A. Ajavakom, H. Norieda, H. Yamada, and Y. Sakata, *J. Phys. Chem. B* 103, 7233 (1999).
66. H. Imahori, S. Ozawa, K. Ushida, M. Takahashi, T. Azuma, A. Ajavakom, T. Akiyama, M. Hasegawa, S. Taniguchi, T. Okada, and Y. Sakata, *Bull. Chem. Soc. Jpn.* 72, 485 (1999).
67. H. Imahori, H. Norieda, Y. Nishimura, I. Yamazaki, K. Higuchi, N. Kato, T. Motohiro, H. Yamada, K. Tamaki, M. Arimura, and Y. Sakata, *J. Phys. Chem. B* 104, 1253 (2000).
68. H. Imahori, T. Hasobe, H. Yamada, Y. Nishimura, I. Yamazaki, and S. Fukuzumi, *Langmuir* 17, 4925 (2001).
69. H. Yamada, H. Imahori, and S. Fukuzumi, *J. Mater. Chem.* 12, 2034 (2002).
70. H. Yamada, H. Imahori, Y. Nishimura, I. Yamazaki, T. K. Ahn, S. K. Kim, D. Kim, and S. Fukuzumi, *J. Am. Chem. Soc.* 125, 9129 (2003).
71. T. Hasobe, H. Imahori, K. Ohkubo, H. Yamada, T. Sato, Y. Nishimura, I. Yamazaki, and S. Fukuzumi, *J. Porphyrins Phthalocyanines* 7, 296 (2003).
72. H. Imahori, H. Norieda, H. Yamada, Y. Nishimura, I. Yamazaki, Y. Sakata, and S. Fukuzumi, *J. Am. Chem. Soc.* 123, 100 (2001).
73. D. Hirayama, K. Takimiya, Y. Aso, T. Otsubo, T. Hasobe, H. Yamada, H. Imahori, S. Fukuzumi, and Y. Sakata, *J. Am. Chem. Soc.* 124, 532 (2002).
74. D. Hirayama, T. Yamashiro, K. Takimiya, Y. Aso, T. Otsubo, H. Norieda, H. Imahori, and Y. Sakata, *Chem. Lett.* 570 (2000).
75. A. Ishida and T. Majima, *Nanotechnology* 10, 308 (1999).
76. N. Terasaki, T. Akiyama, and S. Yamada, *Langmuir* 18, 8666 (2002).
77. T. Akiyama, M. Inoue, Y. Kuwahara, and S. Yamada, *Jpn. J. Appl. Phys.* 41, 4737 (2002).
78. N. Terasaki, T. Akiyama, and S. Yamada, *Chem. Lett.* 668 (2000).
79. O. Enger, F. Nuesch, M. Fibbioli, L. Echegoyen, E. Pretsch, and F. Diederich, *J. Mater. Chem.* 10, 2231 (2000).
80. R. S. Reese and M. A. Fox, *Can. J. Chem.* 77, 1077 (1999).
81. F. B. Abdelrazzaq, R. C. Kwong, and M. E. Thompson, *J. Am. Chem. Soc.* 124, 4796 (2002).
82. A. Ikeda, T. Hatano, S. Shinkai, T. Akiyama, and S. Yamada, *J. Am. Chem. Soc.* 123, 4855 (2001).
83. C. W. Sheen, J.-X. Shi, J. Mårtensson, A. N. Parikh, and D. L. Allara, *J. Am. Chem. Soc.* 114, 1514 (1992).
84. T. Baum, S. Ye, and K. Uosaki, *Langmuir* 15, 8577 (1999).
85. K. Adlkofer, M. Tanaka, H. Hillebrandt, G. Wiegand, E. Sackmann, T. Bolom, R. Deutschmann, and G. Abstreiter, *Appl. Phys. Lett.* 76, 3313 (2000).
86. Y. Gu and D. H. Waldeck, *J. Phys. Chem. B* 102, 9015 (1998).
87. Y. Gu, K. Kumar, A. Lin, I. Read, M. B. Zimmt, and D. H. Waldeck, *J. Photochem. Photobiol. A* 105, 189 (1997).
88. Y. Gu and D. H. Waldeck, *J. Phys. Chem.* 100, 9573 (1996).
89. A. R. Noble-Luginbuhl and R. G. Nuzzo, *Langmuir* 17, 3937 (2001).
90. A. J. Bard, M. Stratmann, and S. Licht Eds., Semiconductor Electrodes and Photoelectrochemistry, "Encyclopedia of Electrochemistry," Vol. 6. Wiley-VCH, Weinheim, 2002.
91. H. Gerischer, *NATO Advanced Study Institutes Series, Series B: Physics* B69, 199 (1981).
92. J. O'M. Bockris and K. Uosaki, *J. Electrochem. Soc.* 125, 223 (1978).
93. A. Fujishima and K. Honda, *Nature* 238, 27 (1972).
94. M. Brust, M. Walker, D. Bethell, D. J. Shiffrin, and R. Whyman, *J. Chem. Soc., Chem. Commun.* 801 (1994).
95. M. Brust, J. Fink, D. Bethell, D. J. Shiffrin, and C. Kiely, *J. Chem. Soc., Chem. Commun.* 1655 (1995).
96. M. J. Hostetler, A. C. Templeton, and R. W. Murray, *Langmuir* 15, 3782 (1999).
97. S. Yamada, T. Tasaki, T. Akiyama, N. Terasaki, and S. Nitahara, *Thin Solid Films* 438–439, 70 (2003).
98. H. Imahori, Y. Kashiwagi, Y. Endo, T. Hanada, Y. Nishimura, I. Yamazaki, Y. Araki, O. Ito, and S. Fukuzumi, *Langmuir* 20, 73 (2004).
99. H. Imahori and S. Fukuzumi, *Adv. Mater.* 13, 1197 (2001).
100. T. Hasobe, H. Imahori, P. V. Kamat, and S. Fukuzumi, *J. Am. Chem. Soc.* 125, 14962 (2003).
101. G. Li, W. Fudickar, M. Skupin, A. Klyszcz, C. Draeger, M. Lauer, and J.-H. Fuhrhop, *Angew. Chem. Int. Ed.* 41, 1828 (2002).
102. M. L. Steigerwald, A. P. Alivasatos, J. M. Gibson, T. D. Harris, R. Kortan, A. J. Muller, A. M. Thayer, T. M. Duncan, D. C. Douglass, and L. E. Brus, *J. Am. Chem. Soc.* 110, 3046 (1988).
103. T. Nakanishi, B. Ohtani, and K. Uosaki, *J. Phys. Chem. B* 102, 1571 (1998).
104. S. Ogawa, F.-R. F. Fan, and A. J. Bard, *J. Phys. Chem.* 99, 11182 (1995).
105. T. Nakanishi, B. Ohtani, and K. Uosaki, *J. Electroanal. Chem.* 455, 229 (1998).
106. T. Nakanishi, B. Ohtani, and K. Uosaki, *Jpn. J. Appl. Phys.* 38, 518 (1999).
107. M. Miyake, T. Torimoto, M. Nishizawa, T. Sakata, H. Mori, and H. Yoneyama, *Langmuir* 15, 2714 (1999).
108. S. Ogawa, K. Hu, F.-R. F. Fan, and A. J. Bard, *J. Phys. Chem. B* 101, 5705 (1997).
109. E. P. A. M. Bakkers, A. L. Roest, A. W. Marsman, L. W. Jenneskens, L. I. De J. Steensel, J. J. Kelly, and D. Vanmaekelbergh, *J. Phys. Chem. B* 104, 7266 (2000).
110. D.-H. Woo, S.-J. Choi, D.-H. Han, H. Kang, and S.-M. Park, *Phys. Chem. Chem. Phys.* 3, 3382 (2001).
111. M. Miyake, T. Torimoto, T. Sakata, H. Mori, and H. Yoneyama, *Langmuir* 15, 1503 (1999).
112. K. Uosaki, M. Okamura, and K. Ebina, *Faraday Discuss.* 125, 39 (2003).
113. D. G. Walter, D. J. Campbell, and C. A. Mirkin, *J. Phys. Chem. B* 103, 402 (1999).
114. D. J. Campbell, B. R. Herr, J. C. Hulteen, R. P. V. Duyne, and C. A. Mirkin, *J. Am. Chem. Soc.* 118, 10211 (1996).
115. W. B. Caldwell, D. J. Campbell, K. Chen, B. R. Herr, C. A. Mirkin, A. Malik, M. K. Durbin, P. Dutta, and K. G. Huang, *J. Am. Chem. Soc.* 117, 6071 (1995).
116. R. Wang, T. Iyoda, D. A. Tryk, K. Hashimoto, and A. Fujishima, *Langmuir* 13, 4644 (1997).
117. R. Wang, T. Iyoda, L. Jiang, D. A. Tryk, K. Hashimoto, and A. Fujishima, *J. Electroanal. Chem.* 438, 213 (1997).
118. H.-Z. Yu, Y.-Q. Wang, J.-Z. Cheng, J.-W. Zhao, S.-M. Cai, H. Inokuchi, A. Fujishima, and Z.-F. Liu, *Langmuir* 12, 2843 (1996).
119. T. Kondo, T. Kanai, and K. Uosaki, *Langmuir* 17, 6317 (2001).

120. M. Jaschke, H. Schönherr, H. Wolf, H.-J. Butt, E. Bamberg, M. K. Besocke, and H. Ringsdorf, *J. Phys. Chem.* 100, 2290 (1996).
121. Z. Liu, C. Zhao, M. Tang, and S. Cai, *J. Phys. Chem.* 100, 17337 (1996).
122. H.-Z. Yu, Y.-Q. Wang, S.-M. Cai, and A.-F. Liu, *Chem. Lett.* 903 (1996).
123. W.-W. Zhang, X.-M. Ren, H.-F. Li, C.-S. Lu, C.-J. Hu, H.-Z. Zhu, and Q.-J. Meng, *J. Colloid Interface Sci.* 255, 150 (2002).
124. K. Tamada, J. Nagasawa, F. Nakanishi, K. Abe, T. Ishida, M. Hara, and W. Knoll, *Langmuir* 14, 3264 (1998).
125. S. W. Han, C. H. Kim, S. H. Hong, Y. K. Chung, and K. Kim, *Langmuir* 15, 1579 (1999).
126. R. Wang, L. Jiang, T. Iyoda, D. A. Tryk, K. Hashimoto, and A. Fujishima, *Langmuir* 12, 2052 (1996).
127. K. Morigaki, A.-F. Liu, K. Hashimoto, and A. Fujishima, *J. Phys. Chem.* 99, 14771 (1995).
128. R. Wang, T. Iyoda, K. Hashimoto, and A. Fujishima, *J. Phys. Chem.* 99, 3352 (1995).
129. K. Morigaki, T. Enomoto, K. Hashimoto, and A. Fujishima, *Mol. Cryst. Liq. Cryst.* 246, 409 (1994).
130. Z. F. Liu, B. H. Loo, R. Baba, and A. Fujishima, *Chem. Lett.* 1023 (1990).
131. A. N. Shipway and I. Willner, *Acc. Chem. Res.* 34, 421 (2001).
132. E. Katz, M. Lion-Dagan, and I. Willner, *J. Electroanal. Chem.* 382, 25 (1995).
133. M. Lion-Dagan, E. Katz, and I. Willner, *J. Am. Chem. Soc.* 116, 7931 (1994).
134. I. Willner, S. Rubin, and Y. Cohen, *J. Am. Chem. Soc.* 115, 4937 (1993).
135. Z. Wang, M. J. Cook, A.-M. Nygård, and D. A. Russell, *Langmuir* 19, 3779 (2003).
136. M. A. Fox, M. O. Wolf, and R. S. Reese, *NATO ASI Series, Series C: Mathematical and Physical Sciences*, 485, 143 (1996).
137. N. Nakashima, T. Nakanishi, A. Nakatani, Y. Deguchi, H. Murakami, T. Sagara, and M. Irie, *Chem. Lett.* 591 (1997).
138. I. A. Banerjee, L. Yu, and H. Matsui, *J. Am. Chem. Soc.* 125, 9542 (2003).
139. M. A. Fox and M. D. Wooten, *Langmuir* 13, 7099 (1997).
140. L.-H. Guo, G. McLendon, H. Razafitrimo, and Y. Gao, *J. Mater. Chem.* 6, 369 (1996).
141. K. M. Roth, J. S. Lindsey, D. F. Bocian, and W. G. Kuhr, *Langmuir* 18, 4030 (2002).
142. S. T. Plummer and P. W. Bohn, *Langmuir* 18, 4142 (2002).
143. S. T. Plummer, Q. Wang, P. W. Bohn, R. Stockton, and M. A. Schwartz, *Langmuir* 19, 7528 (2003).
144. Y. Sato and K. Uosaki, *J. Electroanal. Chem.* 384, 57 (1995).
145. Y. S. Obeng and A. J. Bard, *Langmuir* 7, 195 (1991).
146. W. A. Jackson and D. R. Bobbitt, *Microchem. J.* 49, 99 (1994).
147. Y. Zu and A. J. Bard, *Anal. Chem.* 73, 3960 (2001).
148. W. Miao and A. J. Bard, *Anal. Chem.* 75, 5825 (2003).
149. S. Szunerits and D. R. Walt, *Anal. Chem.* 74, 1718 (2002).
150. L. Zhu, H. Tang, Y. Harima, K. Yamashita, Y. Aso, and T. Otsubo, *J. Mater. Chem.* 12, 2250 (2002).
151. Y. Sato, S. Yabuki, and F. Mizutani, *Chem. Lett.* 1330 (2000).
152. Y. Sato, T. Sawaguchi, and F. Mizutani, *Electrochem. Commun.* 3, 131 (2001).
153. D. H. Reich, M. Tanase, A. Hultgren, L. A. Bauer, C. S. Chen, and G. J. Meyer, *J. Appl. Phys.* 93, 7275 (2003).
154. P. E. Laibinis, J. J. Hickman, M. S. Wrighton, and G. M. Whitesides, *Science* 245, 845 (1989).
155. G. M. Whitesides, J. P. Mathias, and C. T. Seto, *Science* 254, 1312 (1991).
156. N. Matsuda, T. Sawaguchi, M. Osawa, and I. Uchida, *Chem. Lett.* 145 (1995).
157. K. C. Chan, T. Kim, J. K. Schoer, and R. M. Crooks, *J. Am. Chem. Soc.* 117, 5875 (1995).
158. L. F. Rozsnyai and M. S. Wrighton, *J. Am. Chem. Soc.* 116, 5993 (1994).
159. R. Vaidya, L. M. Tender, G. Bradley, M. J. O'Brien II, M. Cone, and G. P. López, *Biotechnol. Prog.* 14, 371 (1998).
160. S. Y. Oh, J. K. Park, C. M. Chung, and J. W. Choi, *Opt. Mater.* 21, 265 (2002).
161. J. C. Love, D. B. Wolfe, M. L. Chabinyc, K. E. Paul, and G. M. Whitesides, *J. Am. Chem. Soc.* 124, 1576 (2002).
162. P. L. Schilardi, O. Azzaroni, and R. C. Salvarezza, *Langmuir* 17, 2748 (2001).
163. L. Pardo, W. C. Wilson, Jr., and A. Boland, *Langmuir* 19, 1462 (2003).
164. M. R. Shadnam, S. E. Kirkwood, R. Fedosejevs, and A. Amirfazli, *Langmuir* 20, 2667 (2003).
165. D. Ryan, B. A. Parviz, V. Linder, V. Semetey, S. K. Sia, J. Su, M. Mrksich, and G. M. Whitesides, *Langmuir* 20, 9080 (2004).
166. S. Sun and G. J. Leggett, *Nano Lett.* 2, 1223 (2002).
167. K. S. L. Chong, S. Sun, and G. J. Leggett, *Langmuir* 21, 3903 (2005).
168. T. Kondo, S. Horiuchi, I. Yagi, S. Ye, and K. Uosaki, *J. Am. Chem. Soc.* 121, 391 (1999).
169. R. Baba, A. Fujishima, K. Hashimoto, and T. Miwa, *Nonlinear Opt.* 22, 497 (1999).
170. S. Nakabayashi, E. Fukushima, R. Baba, N. Katano, Y. Sugihara, and J. Nakayama, *Electrochem. Commun.* 1, 550 (1999).
171. M. Okamura, T. Kondo, and K. Uosaki, *J. Phys. Chem. B* 105, 9897 (2005).
172. M. Aslam, I. S. Mulla, and K. Vijayamohanan, *Langmuir* 17, 7487 (2001).
173. M. W. Holman, R. Liu, and D. M. Adams, *J. Am. Chem. Soc.* 125, 12649 (2003).